ORIGINAL ARTICLE

Amplifying effects of recurrent drought on the dynamics of tree growth and water use in a subalpine forest

Florian Oberleitner[1] | Henrik Hartmann[2] | Roland Hasibeder[1] |
Jianbei Huang[2] | Adriano Losso[3,4] | Stefan Mayr[3] | Walter Oberhuber[3] |
Gerhard Wieser[3,5] | Michael Bahn[1]

[1]Department of Ecology, University of Innsbruck, Innsbruck, Austria

[2]Department of Biogeochemical Processes, Max Planck Institute for Biogeochemistry, Jena, Germany

[3]Department of Botany, University of Innsbruck, Innsbruck, Austria

[4]Hawkesbury Institute for the Environment, Western Sydney University, Richmond, New South Wales, Australia

[5]Department of Alpine Timberline Ecophysiology, Federal Research and Training Centre for Forests, Natural Hazards and Landscape (BFW), Innsbruck, Austria

Correspondence
Florian Oberleitner and Michael Bahn,
Department of Ecology, University of
Innsbruck, Sternwartestraße 15, 6020
Innsbruck, Austria.
Email: Florian.Oberleitner@uibk.ac.at and
Michael.Bahn@uibk.ac.at

Funding information
Österreichische
Forschungsförderungsgesellschaft,
Grant/Award Number: Project LTER-CWN;
Austrian Academy of Sciences,
Grant/Award Number: Project ClimLUC;
Austrian Science Fund, Grant/Award Numbers:
Erwin Schrödinger Fellowship J-4300, P32203

Abstract

Despite recent advances in our understanding of drought impacts on tree functioning, we lack knowledge about the dynamic responses of mature trees to recurrent drought stress. At a subalpine forest site, we assessed the effects of three years of recurrent experimental summer drought on tree growth and water relations of *Larix decidua* Mill. and *Picea abies* (L. Karst.), two common European conifers representative for contrasting water-use strategies. We combined dendrometer and xylem sap flow measurements with analyses of xylem anatomy and non-structural carbohydrates and their carbon-isotope composition. Recurrent drought increased the effects of soil moisture limitation on growth and xylogenesis, and to a lesser extent on xylem sap flow. *P. abies* showed stronger growth responses to recurrent drought, reduced starch concentrations in branches and increased water-use efficiency when compared to *L. decidua*. Despite comparatively larger maximum tree water deficits than in *P. abies*, xylem formation of *L. decidua* was less affected by drought, suggesting a stronger capacity of rehydration or lower cambial turgor thresholds for growth. Our study shows that recurrent drought progressively increases impacts on mature trees of both species, which suggests that in a future climate increasing drought frequency could impose strong legacies on carbon and water dynamics of treeline species.

KEYWORDS

dehydration dynamics, drought legacy effects, stem capacitance, tree line, tree water relations, xylem anatomy, xylem sap flow

1 | INTRODUCTION

Trees are exposed to an increasing risk of drought stress due to the recent and projected rise in the frequency and severity of drought events (C. D. Allen et al., 2010; Büntgen et al., 2021; IPCC, 2018). Drought effects on trees can range from short-term impacts, such as reduced carbon (C) uptake and/or growth during a drought event (Bréda et al., 2006; Eilmann et al., 2006; Rennenberg et al., 2006), to long-lasting legacies (Müller & Bahn, 2022; Schwalm et al., 2017), including multi-year growth reductions (Anderegg et al., 2015) and increased mortality (Adams et al., 2017; C. D. Allen et al., 2010) after drought. Tree functioning can be increasingly impaired by repeatedly occurring drought events (Kannenberg et al., 2020) and drought legacies may also lead to increased vulnerability to subsequent drought events (Kannenberg et al., 2020; Menezes-Silva et al., 2019; Peltier & Ogle, 2019; Rennenberg et al., 2006), especially if time between droughts does not sufficiently allow for recovery (Schwalm et al., 2017). However, susceptibility of trees and forests to recurrent drought is highly variable among species (Anderegg et al., 2020) and the underlying mechanisms are not well understood. This is related to the fact that multi-year datasets are largely restricted to tree rings and thus provide only low temporal resolution information on drought responses of tree radial growth. Furthermore, the quantification of drought effects in tree-ring studies is based on assumptions of tree growth under different non-drought conditions (Kannenberg et al., 2020). To understand and consistently quantify drought effects on growth and water-use dynamics, experimental studies are needed (Grams et al., 2021; Zuidema et al., 2018), yet most available experiments to date have been performed on young saplings in non-natural growing environments, such as potted plants in greenhouses or common garden setups (Hartmann, Moura, et al., 2018). However, drought responses can differ strongly depending on tree age or size, which limits the possibility of transferring observations on saplings to mature trees (Andivia et al., 2020; Bennett et al., 2015; Cavender-Bares & Bazzaz, 2000; Hanson et al., 2001; Hartmann, Adams, et al., 2018). Most information on mature tree drought responses come from studies of natural drought events in drought-prone regions or drought experiments performed in (semi-)arid regions (e.g., Adams et al., 2015; Gaylord et al., 2013; McDowell et al., 2019; Plaut et al., 2012). In contrast, trees growing at sites with previously ample water supply might be particularly vulnerable to intense and/or recurrent drought due to a lack in drought adaptation (Blumstein et al., 2020; Isaac-Renton et al., 2018). Furthermore, there is increasing evidence that, as a result of ongoing climate change, drought severity and frequency are increasing in regions that were previously largely unaffected by drought, including large parts of the Alps (Büntgen et al., 2021; Calanca, 2007; Gobiet et al., 2014; Moravec et al., 2021; Spinoni et al., 2018), increasing potential risks also for mountain forests (Albrich et al., 2020). The twofold rise in temperatures in many mountain regions, compared to global average (Gobiet et al., 2014; Pepin et al., 2015; Rangwala & Miller, 2012), has also led to increased evapotranspiration and water vapour pressure deficits (VPD), which accelerate and amplify drought stress (Grossiord et al., 2020; Sangines

de Carcer et al., 2018). Because an increase in drought frequency, severity and spatial extent has the potential to ultimately cause persistent shifts in species composition, forest dynamics and stand structure (McDowell et al., 2020; Trugman et al., 2020), it is of major importance to better understand the effects of recurrent drought on tree functioning and to resolve the mechanisms on mature trees in their natural environment.

Next to drought responses of radial growth and xylem sap flow, the effects of drought on stem shrinking and swelling dynamics provide major insights into the processes underlying tree functioning under water limitation (Mencuccini et al., 2013; Peters et al., 2021; Steppe et al., 2015; Zweifel, 2016; Zweifel et al., 2006). Dehydration occurs when water gets withdrawn from the inner bark to maintain transpiration during periods of high evaporative demand (Zweifel et al., 2001). It can be strongly enhanced under reduced plant water status at low soil water availability (Sevanto, 2018; Steppe et al., 2015). Under such conditions, reduced turgor and increased phloem sap viscosity impair phloem functioning (Sevanto, 2014, 2018). Simultaneously, a low water availability in the vascular cambium limits cell formation due to decreased turgor for cell expansion and proliferation (Cabon et al., 2020; Körner, 2003; Zweifel, Haeni, et al., 2016). While there is increasing evidence that cambium and phloem hydration play a major role under lethal drought (Lamacque et al., 2020; Preisler et al., 2021), the sensitivity of these tissues to dehydration is still largely unknown. Knowledge about dehydration dynamics and sensitivity could strongly contribute to understanding how tree functioning is limited under drought (Martinez-Vilalta et al., 2019) and may help explain why drought responses differ between species.

Here, we aimed to determine growth and water-use response dynamics of mature trees to identify key limitations for tree functioning under recurrent drought at a subalpine forest, a site previously unaffected by severe drought events. We subjected mature trees from two major coniferous species in the European Alps, deciduous European larch (*Larix decidua* Mill.) and evergreen Norway spruce (*Picea abies* L. Karst.), to 3 years of recurrent (i.e., annually repeated) experimental summer drought followed by typical wet winter seasons. While sharing similar hydraulic characteristics (Charra-Vaskou et al., 2011; Rosner et al., 2019), the two species represent contrasting water-use strategies that are reflected by a deep versus shallow rooting system (Schmid & Kazda, 2002; Valentini et al., 1994) as well as an exploitative versus conservative stomatal behaviour (Anfodillo et al., 1998; Leo et al., 2014), respectively. In consequence, *L. decidua* has been associated with a lower drought vulnerability than *P. abies* (Anfodillo et al., 1998; Hartl-Meier et al., 2014). We quantified radial and shoot elongation growth and xylem anatomy, xylem sap flow, diel stem radius variations as a proxy for tree water status and stem electrical resistivity as a proxy for xylem water content. Furthermore, we analysed leaf and branch non-structural carbohydrate (NSC) concentrations and carbon isotope composition of soluble sugars (δ^{13}C) as a measure for tree carbon status and intrinsic water-use efficiency. We tested the hypotheses that (i) drought affects key parameters of tree carbon and water relations (including growth dynamics, wood anatomical traits, stem

tissue hydration dynamics, xylem sap flow, NSC concentrations and intrinsic water use efficiency) more strongly for *P. abies* than for *L. decidua*, and (ii) recurrent summer drought amplifies negative drought impacts on these parameters and enhances the differences between the two species.

2 | MATERIALS AND METHODS

2.1 | Study site and experimental design

The subalpine forest site is situated in the Austrian Central Alps at the long-term ecological research (LTER) master site Stubai valley (47°07′34″N, 11°17′42″E). The site is situated on a south–southeast exposed slope between 1960 and 2000 m.a.s.l., with an inclination of 20–35°. Mean annual temperature and mean annual precipitation are 3°C and 1097 mm, respectively (Bahn et al., 2006; Schmitt et al., 2010). The area was formerly used as a pasture and upon abandonment was reforested in the early 1980s. It is dominated by the deciduous coniferous tree species European larch (*Larix decidua* Mill.) and the evergreen species Norway spruce (*Picea abies* L. Karst.). Trees form an open stand with a minor portion of Swiss stone pine (*Pinus cembra* L.) and Swiss mountain pine (*Pinus mugo* Turra), and an understory vegetation dominated by graminoids and forbs typical of the nearby grasslands (Schmitt et al., 2010) with a few dwarf shrubs (*Vaccinium* spp.). Soils are dystric cambisols on siliceous and calcareous bedrock as in an adjacent abandoned grassland (Meyer et al., 2012). Field capacity and permanent wilting point of the soils are at 46.8 and 23 vol%, respectively, determined using HYPROP evaporation method (HYPROP 2, Meter Group).

Three drought plots and three control plots were established in 2015, each plot covering an area of ~230 m². (Supporting Information: Figure S1). In the centre of each plot, two individual trees of each *L. decidua* and *P. abies* were located, resulting in a total of 24 studied trees (six trees per species and treatment). Tree size and stand characteristics did not differ significantly between treatments and within species at the beginning of the experiment (Table 1). Trees were subjected to sustained and recurrent summer drought by excluding 100% of the precipitation in the drought plots up to 4 months during the main growing season in 2016, 2017 and 2018 (Table 2). The exact timing of the treatment depended on weather conditions that determined site accessibility for shelter installation and removal in spring and autumn, respectively. To exclude precipitation, semi-transparent ripstop plastic

sheets were mounted 1.3 m above ground on manually constructed wooden racks, where precipitation would run off without affecting other plots. Plastic sheets were mounted tight on the stems and sealed to prevent stem runoff and avoid throughfall precipitation. While the wooden constructions were left installed also during winter, plastic sheets were removed each year at the end of each growing season. To prevent subsurface water flow from entering the drought plots, 1.5 m deep trenches were installed upslope of the drought plots. The distance of these trenches from the stems of the studied trees was at least three times the radius of their respective crowns in all plots. Therefore, and due to a lack of lateral trenches, the root system of study trees was not considered to have been significantly damaged by trenching. Trenches were laid out with plastic sheets to evacuate water to the outsides of the plots and refilled with excavated soil. Trenches remained permanently installed, thus soil water content (SWC) recovered mainly through water input from precipitation. Because trees were potentially able to access some small amount of water from the untrenched areas adjacent to the rainout shelters, the treatment likely underestimated drought effects as recently shown for many drought experiments when compared to natural droughts (Kröel-Dulay et al., 2022).

2.2 | Microclimate

In one control and one drought plot each, a micrometeorological station was set up to measure air temperature (T_a) and relative humidity (RH; both Vaisala HMP45AC) in the open 2 m above ground. Furthermore, SWC (SM150T, Delta-T Devices Ltd) was measured at 5, 10, 20, 40 and 80 cm soil depth. Measured values were averaged and logged at 30 min intervals using CR1000 data loggers (Campbell Scientific). Precipitation (P) measurements were taken from a meadow study site (Schmitt et al., 2010) located within a distance of 800 m to avoid measurement artefacts by needles plugging the rain gauge (Model 52202, R. M. Young Company). VPD was calculated from T_a and RH following R.G. Allen et al. (1998).

2.3 | Dendrochronological and wood anatomy analysis

In spring 2019, two radii per tree were extracted from opposite sides of the stem at 0.5 m height using an increment borer. Trees were

TABLE 1 Mean ± 1 SE tree characteristics (stem diameter, stem perimeter and crown diameter) and plot characteristics (stand height, soil depth) as assessed in 2015 (*n* = 6 trees per species and treatment, *n* = 3 plots per treatment)

Treatment	Species	Stem diameter (cm)	Stem perimeter (cm)	Crown diameter (m)	Stand height (m)	Soil depth (cm)
Control	*Larix decidua*	18.05 ± 1.01	56.70 ± 3.19	5.00 ± 0.26	7.00 ± 0.37	36.67 ± 3.80
	Picea abies	16.13 ± 1.60	50.65 ± 5.02	4.00 ± 0.34		
Drought	*Larix decidua*	18.88 ± 1.47	59.32 ± 4.65	4.58 ± 0.38	6.67 ± 0.46	38.33 ± 2.10
	Picea abies	17.40 ± 1.46	54.65 ± 4.60	3.92 ± 0.15		

Note: Differences between treatments were not significant (*p* > 0.5).

cored parallel to the contour to avoid biases induced by formation of reaction wood. In the laboratory, increment cores were air-dried, mounted on grooved boards and the surface was prepared with a sharp razor blade to produce flat surfaces. For contrast enhancement of tree-ring boundaries, white chalk powder was rubbed into the tracheid-lumen (Pilcher, 1990). Ring widths were measured to the nearest 1 µm using a light microscope (Olympus SZ61) fitted with a LINTAB measuring system (Frank Rinn). Correct dating of measured time series of ring width were checked with COFECHA software (Holmes, 1983) and individual ring-width chronologies were developed for each individual tree. To account for pre-treatment differences in tree radial growth, tree ring width during the study period 2016–2018 was analysed for each individual tree and year in relation to mean tree ring width in a 5-year period before the treatment started (2011–2015). To assess drought effects on xylem formation, the average number of cell rows per tree ring, corresponding to annual cell formation rate, was measured for the 3 study years (2016–2018). Mean radial cell diameter as a proxy for cell enlargement was calculated as the quotient of tree ring width and the number of cell rows formed in the corresponding year.

2.4 | Dendrometer measurements

All trees were equipped with high-resolution circumference band dendrometers (DC2, Ecomatik GmbH), which were installed in 2015, 1 year before the beginning of the drought treatment. We mounted dendrometers at a height of 150 cm above ground on the north facing side of the stem to minimise radiation effects on the sensors. Part of the dead outermost layers of the bark was removed before installation to minimise the influence of hygroscopic shrinking and swelling on dendrometer records. Data were logged in 15 min intervals by HOBO UX120-006M analogue data loggers (Onset Computer Corporation). Stem circumference data were converted to stem radius data, which we subsequently used to calculate diurnal radius variations, maximum daily stem shrinkage (MDS) and TWD following Zweifel (2016) and Dietrich, Zweifel, Kahmen (2018). Daily values for TWD were calculated as the difference between the daily maximum radius in the morning and its preceding maximum radius reading, indicating overall water deficit-related stem shrinkage. Daily values for MDS, as an indicator of diurnal water deficit related stem shrinkage, were calculated as the difference between the maximum radius before the onset of stem shrinkage in the morning, corresponding to the maximum expansion of the stem due to growth, water refilling and saturation, and the minimum radius during the day, corresponding to maximal diurnal depletion of water stored in the stem. Monthly averages of MDS and diurnal stem radius variations were subsequently calculated for each individual tree.

Additionally, growth models were fit to the dendrometer-derived annual stem radius change data for each individual tree and year to estimate the date of the onset of radial growth (GRO$_{start}$), date of maximum growth rate and maximum growth rate (dGRO$_{max}$ and GRO$_{max}$, respectively) and the date of the end of radial growth

(GRO$_{end}$) following the approach of Kahm et al. (2010) and Paine et al. (2012). In short, Gompertz and logistic growth functions were fit to the data and the better model fit was chosen based on Akaike Information Criterion (AIC) evaluation for analysis of the growth curve. Growth parameters were calculated as the x-axis intercept of the tangent of the inflection point (GRO$_{start}$), the date at the inflection point (dGRO$_{max}$), the slope at the inflection point (GRO$_{max}$) and the point of interception of the upper asymptote and the tangent of the inflection point (GRO$_{end}$) of the growth curve.

2.5 | Shoot growth

Shoot growth was repeatedly assessed at four time points during the growing season of 2018 (Supporting Information: Figure S6). For each tree, five south-exposed shoots were selected and marked before the onset of shoot growth and were measured at each of the four time points using a digital caliper gauge. For statistical analyses the mean values per tree were used.

2.6 | Sap flow

All 24 studied trees were equipped with a set of tissue heat balance sap flow sensors (EMS 51, EMS Brno, Brno, CZ; described in detail by Čermák et al. [2004]). Sensors were mounted at a height of ~100 cm above ground at the south facing side of the stem before the beginning of the treatment in 2016. To prevent confounding heating effects from solar radiation, sensors and the surrounding tissue were protected with aluminium-faced foam insulation covers provided with the EMS 51 sap flow system. Xylem sap flow rates (l h^{-1}) were measured in 10 s intervals and 15 min averages were recorded by the EMS 51 data logger.

2.7 | Electrical resistivity tomography

To estimate effects of drought on water distribution in stem xylem, electrical resistivity measurements were performed on three P. abies trees per treatment at peak drought in the third study year (end of September 2018). A set of nails (length 5 cm) was installed around the trunk circumference at 24 measuring points, 40 cm above the ground (see Bär et al., 2019; Ganthaler et al., 2019; Losso et al., 2020). Nails were installed with equal distance to each other (counterclockwise numbering with north orientation of measuring point 1), until contact to the sapwood was established. Tree geometry and positions of measuring points were determined with an electronic caliper (PiCUS Calliper Standard Version, Argus Electronic Gmbh) and processed using the PiCUS Software (PiCUS Q73, Argus Electronic Gmbh). Nails were connected to a 24-channel resistivity system (PiCUS: Tree-Tronic, Argus Electronic Gmbh) and electrical voltages (voltage levels between 2 and 4) were applied systematically to all measuring points (overall duration of measurements was less than 5 min). For each

tree, a tomogram was generated using a dedicated software, which calculates the cross-sectional distribution of electrical resistivities and spatially distribute them using an inversion scheme based on a finite element simulation operating with regularly arranged tetrahedrons (see Günther, 2004; Günther et al., 2006; Rücker et al., 2006). Tomograms are based on triangle areas, where each triangle was coloured according to its resistivity for a better visualisation of patterns. To analyse tomography data, stem resistivity values were binned and averaged in 10 sections along the radius, each section spanning 10% intervals of the radius from the stem centre (1st decile) to the stem periphery (10th decile). To account for effects of the chosen plots in the statistical analysis, a random intercept for plots was included in the regression model as described in the data analysis section below.

2.8 | NSC and their δ¹³C

Three shoots per individual tree were sampled and pooled at the onset of drought (June) and at peak drought (i.e., immediately before the end of the drought treatment in September) in 2018 to measure NSC concentrations and analyse δ¹³C of soluble sugars, as an indicator of intrinsic water-use efficiency (Francey & Farquhar, 1982). For samples of *L. decidua* taken at the onset of drought 2018, no leaves were available, as samples were taken before leaf out. Needles and branches were separated and ground to fine powder using a ball mill (Retsch MM400). Soluble sugars and starch were extracted following the protocol of Landhäusser et al. (2018). Briefly, approximately 30 mg of fine powders were extracted with 1 ml of 85% ethanol, vortexed for 1 min, incubated at 90°C for 10 min, and centrifuged at 13 000g for 1 min. The supernatant was collected, diluted and analysed for glucose, sucrose, and fructose using a high-performance liquid chromatography coupled to a pulsed amperometric detection (HPLC-PAD). The remaining pellet was washed by 85% ethanol twice, dried and digested with 1.0 ml of sterilised water containing 600 units of α-amylase, vortexed for 1 min, incubated at 85°C for 30 min, and then centrifuged at 13 000g for 1 min. An aliquot of supernatants was collected and digested with amyloglucosidase (Sigma-Aldrich), incubated at 55°C for 30 min, and analysed for glucose hydrolysate using HPLC-PAD. Starch was calculated as glucose equivalents multiplied by a factor of 0.9.

An aliquot of the ethanol extracts was pipetted into a tin cup, dried at 40°C and analysed for δ¹³C using a Finnigan Delta Plus XL EA-IRMS (Thermo Finnigan GmbH) coupled with an autosampler (Huang et al., 2019). We used the δ¹³C of ethanol extracts as a reliable proxy for the δ¹³C of soluble sugars, as has been previously shown in *Pinus sylvestris* (Brandes et al., 2006).

2.9 | Data analysis

All calculations and statistical analyses were performed in R Statistical software (R Development Core Team, 2020) and RStudio (RStudio

Team, 2020), strongly employing R packages 'lubridate' (Grolemund & Wickham, 2011) and 'tidyverse' (Wickham et al., 2019).

The effect of the drought treatment on all parameters, except xylem sap flow (see below), was estimated using robust Bayesian multi-level linear regression models, implemented in Stan modelling software (Stan Development Team, 2020) using R package 'brms' (Bürkner, 2017). The linear model included the respective parameter as the response variable and treatment as the predictor variable. Variation between plots was accounted for by allowing the intercept to vary by plots. In addition, residual standard deviation of the response distribution was predicted from and thereby allowed to vary by treatment (including a random plot intercept) to account for unequal variances between treatments (Bürkner, 2018). We chose the t distribution as the response distribution, which is assumed to be more robust to outliers than normal distribution (J. K. Kruschke, 2013). Please note that count data (number of cells in tree rings) was modelled using a Poisson distribution. Hence, the following model was established:

$$y_i \sim T(v, \mu_i, \sigma_i),$$
$$\mu_i = \beta_{plot[i]} + \beta_t{}^*treatment_i,$$
$$\sigma_i = \gamma_{plot[i]} + \gamma_t{}^*treatment_i,$$

where y_i denotes the ith observation of the corresponding response variable, sampled as random draws from a t-distribution (T) with v degrees of freedom, mean μ_i and standard deviation σ_i. $\beta_{plot[i]}$ and $\gamma_{plot[i]}$ denote plot-specific intercepts, β_t and γ_t denote treatment coefficients and $treatment_i$ denotes the treatment (control, drought) as the explanatory variable. Weakly informative priors (i.e., Normal distribution with mean = 0 and standard deviation = 5) were chosen for treatment coefficients to ensure unbiased estimates of treatment coefficients but still provide a minimum level of regularisation. For all other parameters, default priors from the 'brms' package were used. We ran four Markov-Chain-Monte-Carlo chains with 4000 iterations each (half of which were warm-up runs) to ensure chain convergence. The number of iterations was increased to 10 000 in a few cases where chains did not converge after 4000 iterations. Convergence of the MCMC chains was evaluated using visual inspection of trace plots and Gelman-Rubin statistic (Rhat < 1.01) (Brooks & Gelman, 1998; Gelman & Rubin, 1992). Furthermore, model fits were evaluated with graphical posterior predictive checks. Models were run separately for each species. Values reported in this manuscript are median and 95% credible intervals (95% highest density interval) of the posterior distribution of the treatment covariate. Additionally, the posterior probability that the treatment effect is positive or negative and lies above or below the region of practical equivalence around the null value (ROPE; defined here following the suggestion of J. Kruschke [2014] and J. K. Kruschke [2018] as the standard deviation of 0.1 from the null value, which corresponds to half of a small effect size according to Cohen [1988]) is reported in this manuscript as the posterior probability of direction (pp; Makowski et al., 2019).

To assess xylem sap flow response to VPD, a generalised additive mixed model (GAMM) was fit to the data separately for each species, treatment and month in the corresponding study year. The model was fit to xylem sap flow as the response variable, with VPD

(including a separate cubic regression spline for each treatment) and treatment as the predictor variables, as well as a random intercepts and slopes for tree nested in plot. To account for heterogeneity of variances, the models were fit with a fixed variance structure accounting for an increase in residuals as VPD increases (Zuur et al., 2009). Because VPD was recorded in 30 min intervals, xylem sap flow data, which were recorded in 15 min intervals, were aggregated to half hourly means for the GAMM. We assumed that stomatal responses to VPD are negligible during nighttime and therefore excluded data between 20:00 and 06:00 h.

To evaluate overall relationships of all studied parameters, PCA was performed separately for the two species on data gathered during peak drought in 2018, where most parameters were measured in close temporal proximity. As input variables, annual values were taken for radial increment, shoot length, day when radial growth stopped and xylem anatomical parameters. For NSC, data sampled at peak drought (September) were used. Time series data were aggregated to mean daily maximum xylem sap flow and mean daily stem radius shrinkage of a 1-week period during peak drought when NSC samples were collected.

3 | RESULTS

3.1 | Microclimate and treatment effects on soil water availability

The rain-exclusion treatment strongly reduced SWC in all 3 study years when compared to control, reaching levels close to the permanent wilting point in 2016 and 2017 and levels below the permanent wilting point in 2018 (Figure 1g–i, Supporting Information: Figure S2; Supporting Information: Table S1). SWC progressively decreased with treatment duration, remained low across the whole soil profile for several weeks after the treatment ended, and fully recovered only during winter (Supporting Information: Figure S2). Air temperature, RH and VPD were in a similar range in the 3 study years, whereas precipitation was lower in 2018 when compared to 2016 and 2017 (Supporting Information: Figure S3; Table 2, Supporting Information: Table S1), which resulted in comparatively lower SWC from early August 2018 onwards in both treatments (Figure 1i, Supporting Information: Figure S2).

3.2 | Tree growth and anatomy

Radial growth was reduced under drought in both species and the drought effects increased under recurrent drought (Figure 1a–f, Supporting Information: Figures S4 and S5; Supporting Information: Table S2). Under drought radial growth of *L. decidua* was only slightly reduced in 2016, but strongly reduced by 33.6% (pp = 1) and 35.4% (pp = 0.96) in 2017 and 2018, respectively. In *P. abies*, growth remained unaffected by drought in 2016, but progressively decreased by 26.1% (pp = 0.94) and 38.6% (pp = 1) when compared

to control trees in 2017 and 2018, respectively. In *L. decidua*, annual radial growth ended earlier under drought than in control trees in the second year (2017; pp = 0.97) and third year of the drought treatment (2018; pp = 0.98) (Figure 2a). *P. abies* trees exposed to drought stopped radial growth significantly earlier than control trees in all study years and the effects increased with recurrent drought (Figure 2a; pp ≥ 0.99). We did not find any relevant effects of drought on the date of growth onset, the maximum growth rate and the date at which the maximum growth occurred. Throughout the third year of drought, shoot growth was unaffected by drought in *L. decidua*, but consistently reduced in *P. abies* (pp > 0.97), the length of newly formed shoots declining by 34% relative to control trees (Supporting Information: Figure S6).

Xylem cell formation was more limited by drought in *P. abies* across all years, but hardly affected in *L. decidua* (Figure 2b–d; Supporting Information: Table S2). The number of cell rows formed per year was increasingly reduced in the second and third year of drought in drought exposed trees of both species when compared to the respective control trees (Figure 2b). However, a reduced average radial cell width (Figure 2c) and an increased number of cells per mm increment (Figure 2d) indicate that only in *P. abies* cell expansion was significantly impaired by drought in 2017 and 2018. In contrast, radial cell width showed no response in *L. decidua*.

3.3 | Tree water relations

In both species, diel stem radius dynamics and the resulting maximum daily stem shrinkage (MDS) increased already at the onset of the first drought and remained strongly increased throughout the period of rain-exclusion in each year (pp > 0.98; Figure 3; Supporting Information: Table S3). Daily stem radius shrinkage, as an indicator of stem water depletion, was increased in drought exposed trees already from early morning (i.e., at the start of transpiration) and persisted throughout the whole day so that stems did not fully recover their full radius towards the end of the day under drought. The relative difference in MDS between treatments was stronger in *L. decidua*, which was mainly an effect of lower MDS of *L. decidua* control trees when compared with *P. abies* control trees (Supporting Information: Table S4). This effect was specifically pronounced in the warm and dry month of August 2018, when SWC was comparatively low also in control plots (Figure 1i, Supporting Information: Figure S2) and MDS of control trees of *P. abies* reached levels of drought trees. In consequence, no significant treatment effect was observed in this species. Additionally, overall TWD of drought-exposed trees increased in both species as drought progressed in all study years and both species showed the strongest response in the last year of drought in 2018 (Supporting Information: Figure S7).

Xylem sap flow of both species was strongly related to VPD and saturated at intermediate levels of VPD (Figure 4; Supporting Information: Table S5), when stomatal closure likely balanced increased evaporative demand. In *P. abies*, xylem sap flow of drought-exposed trees tended to be reduced at higher VPD levels
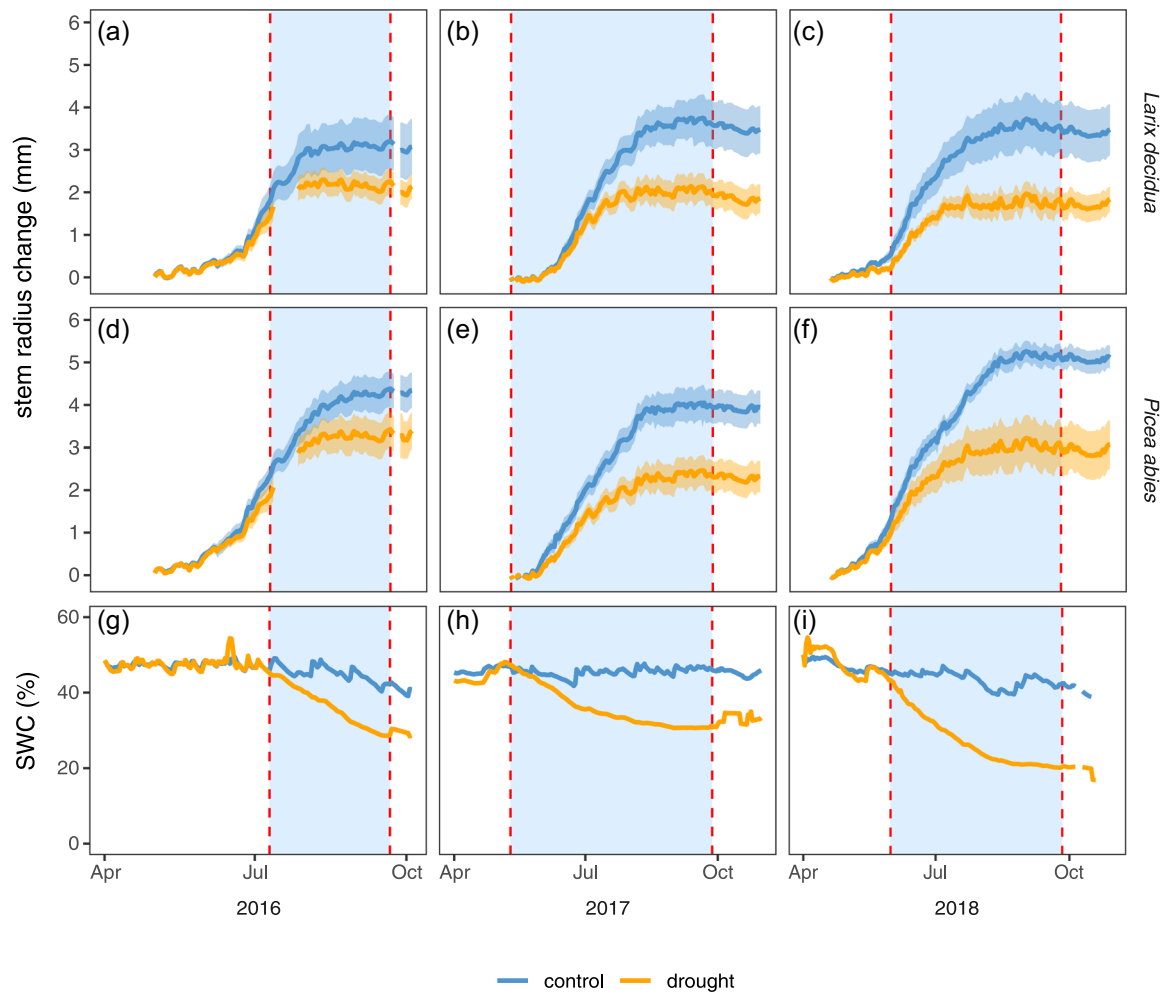
FIGURE 1 Stem radius variations (a–f) for *Larix decidua* (a–c) and *Picea abies* (d–f) and mean volumetric soil water content (SWC; g–i) in the growing periods of the 3 study years 2016, 2017 and 2018. (a–f) Lines and background shadings indicate mean ± 1 SE for stem radius variations (*n* = 6 trees per species and treatment). For SWC (g–i), solid lines represent SWC averaged over the sensors in 5, 10, 20, 40 and 80 cm soil depth (see Supporting Information: Figure S2, for SWC of individual soil depths). Colours denote treatment (blue = control, orange = drought). Background ribbons indicate periods when rainout shelters were closed.

TABLE 2 Duration of the rain exclusion treatment, annual precipitation and precipitation during the rain-exclusion period in the 3 study years 2016–2018

Year	Rain exclusion period	Duration of treatment (days)	Annual precipitation (mm)	Precipitation during rain-exclusion period (mm)
2016	10.07–21.09	73	1100	411
2017	10.05–27.09	140	1330	929
2018	31.05–26.09	118	876	433

third year of drought, xylem sap flow at a given VPD was persistently reduced for both species already from the onset of drought, with most pronounced effects in September 2018 for *L. decidua* and in August 2018 for *P. abies* ($p < 0.04$).

Furthermore, drought increased stem electrical resistivity in *P. abies* at peak drought in 2018 (Figure 5), which reflects a decrease in stem water content (Bär et al., 2019). Under drought, electrical resistivity increased particularly from the third to the ninth decile from the stem centre ($pp > 0.9$; Table S6), indicating an increasing area of dehydrated xylem in the centre of the stem.

3.4 | NSC and their δ¹³C

Concentrations of non-structural carbohydrates (NSC) studied in the third experimental year (2018) showed no clear drought response in *L. decidua* (Figure 6, Supporting Information: Figure S8; Supporting
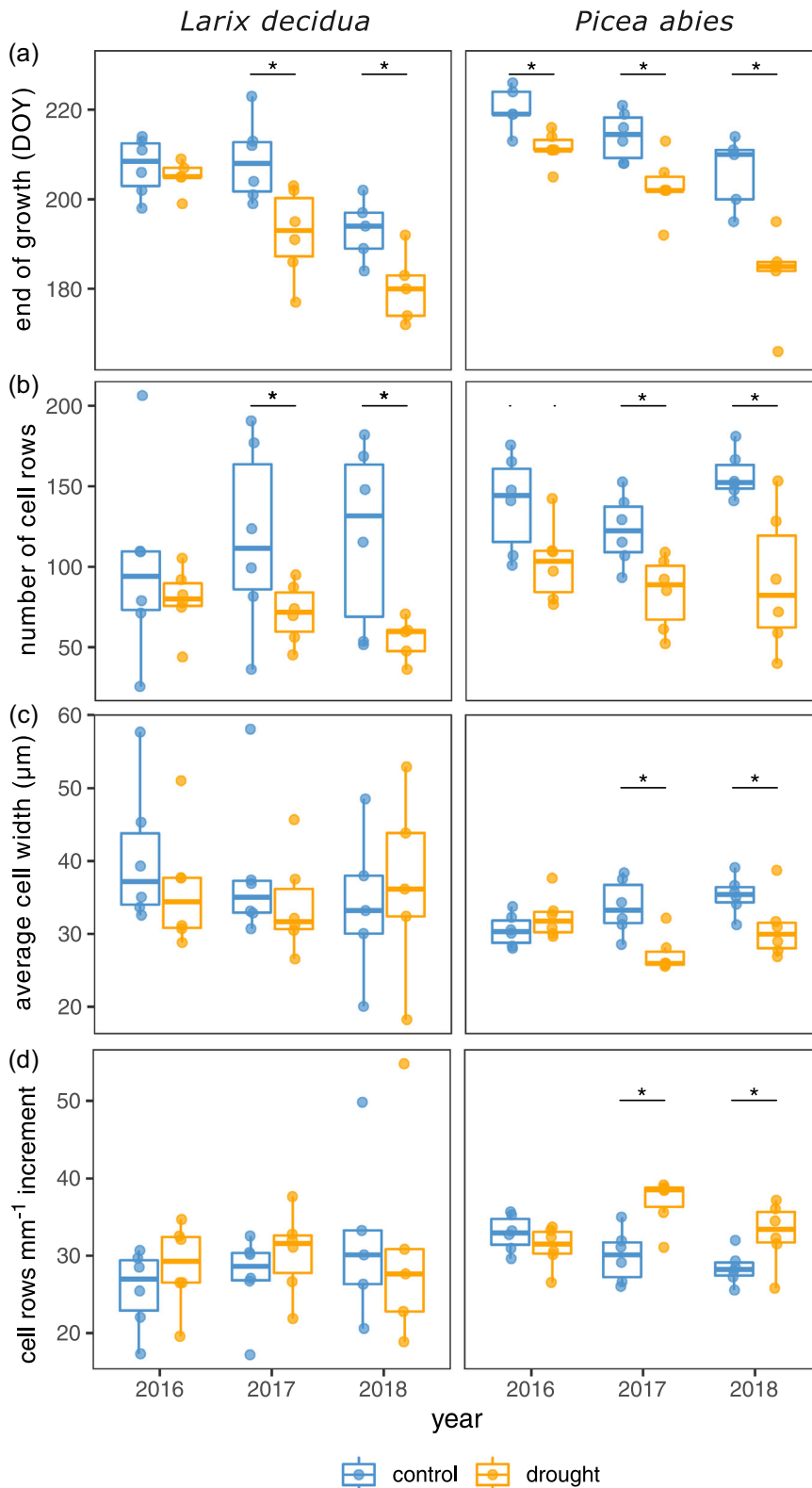
towards the end of the drought treatment in 2016 but showed no clear drought response in 2017. In contrast, in *L. decidua* the drought treatment showed no effects on xylem sap flow in 2016, but a gradual decrease in sap flow with drought progression could be observed in 2017 when compared with control trees. During the

FIGURE 2 Different measures related to radial growth and xylem anatomy for *Larix decidua* (left) and *Picea abies* (right). (a) Day of year (DOY) at which tree growth ended in the corresponding year; (b) number of cell rows measured in radial direction per total tree ring; (c) average radial cell width (μm); (d) average number of cell rows measured in radial direction per mm increment. Boxplots denote median (bold horizontal line), 25th and 75th quartile (box) and 1.5 * interquartile range (whiskers). Points represent individual observations. Colours denote treatment (blue = control, orange = drought). Asterisks and plus signs indicate differences between treatments with a posterior probability >0.95 and >0.9, respectively (*n* = 6 per species and treatment). [Color figure can be viewed at wileyonlinelibrary.com]

Information: Table S7). In drought exposed *P. abies* trees, soluble sugar concentrations tended to be higher in branches and needles of drought-exposed trees already at the onset of drought (*pp* > 0.91) and at peak drought (*pp* > 0.89; Figure 6a,c), but concentrations increased less between drought onset to peak drought when compared to control trees (Supporting Information: Figure S8). Total NSC concentrations tended to be higher in branches and needles of drought exposed trees already at the onset of drought (*pp* > 0.9). However, the magnitude of NSC accumulation during the growing season differed between treatments only in branches, but not in
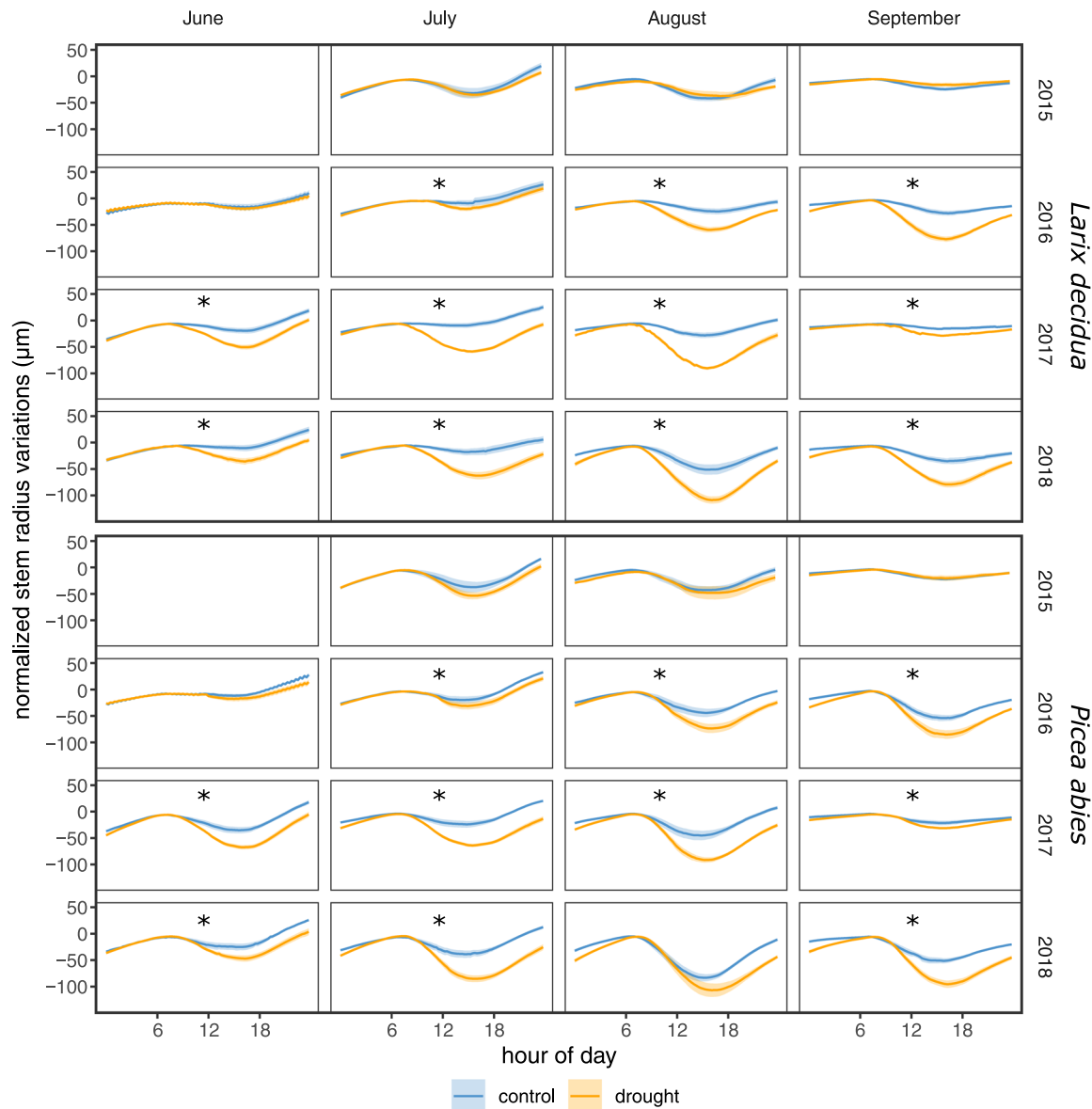
FIGURE 3 Normalised mean diel (0–24 h) stem radius variations (µm) during the summer months in the pre-treatment year 2015 and drought treatment years 2016–2018 for *Larix decidua* (upper panels) and *Picea abies* (lower panels). Lines and shadings represent mean ± 1 SE. Values were normalised to maximum radial expansion in the morning, before shrinkage occurred. Asterisks indicate differences in maximum daily shrinkage (MDS) between treatments with a posterior probability >0.95 (*n* = 6 per species and treatment). [Color figure can be viewed at wileyonlinelibrary.com]

needles (Supporting Information: Figure S8). At peak drought, starch concentration was reduced in the branches by 35.2% (*pp* = 1), but not the in needles of *P. abies* (Figure 6b), which was also reflected in a higher decrease in starch and lower increase in total NSC between onset of drought and peak drought (*pp* > 0.97; Supporting Information: Figure S8).

Furthermore, $\delta^{13}C$ of soluble sugars sampled in 2018 was analysed to estimate drought effects on water-use efficiency. In both species, $\delta^{13}C$ of soluble sugars was higher already at the onset of drought in drought-exposed trees compared to control trees (Figure 7), indicating increased water-use efficiency. In *P. abies*, $\delta^{13}C$ levels remained higher also at peak drought, but $\delta^{13}C$ levels did not change strongly between drought onset and peak drought within

treatments. In drought-exposed *L. decidua*, $\delta^{13}C$ of needles was also higher at peak drought. $\delta^{13}C$ in branches of control trees increased from drought onset towards peak drought and, therefore, no difference between treatments was observed in branches at peak drought for *L. decidua*.

3.5 | PCA of all parameters in response to drought

To evaluate overall relationships between parameters in response to recurrent drought, a PCA was performed for each species on all parameters sampled in 2018 (Supporting Information: Figure S9). Control and drought treatments were clearly separated along with
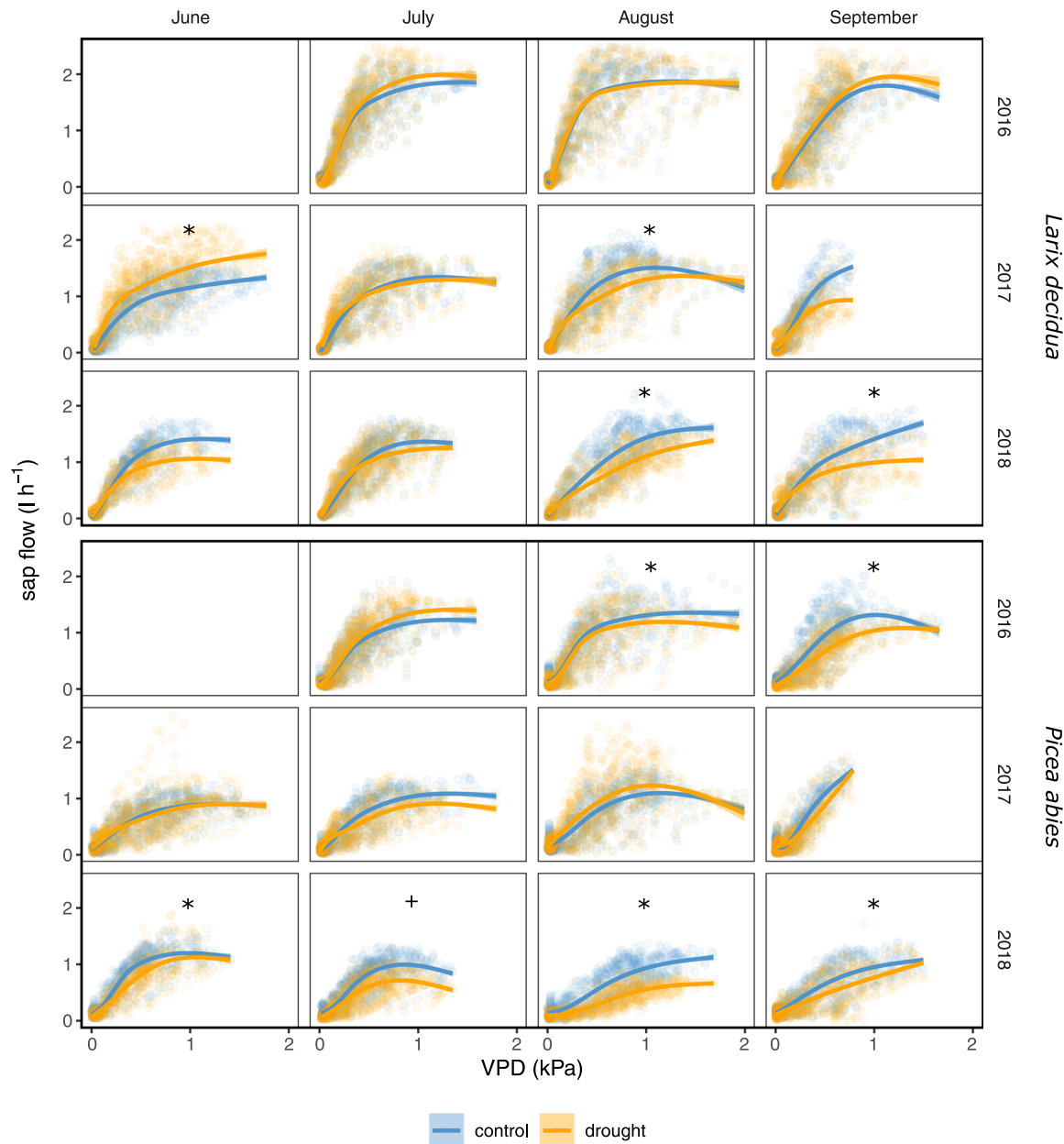
FIGURE 4   Response of xylem sap flow to vapour pressure deficit (VPD) during the summer months of 2016–2018. Response curves show generalised additive model (GAM) fits for the species *Larix decidua* (upper panels) and *Picea abies* (lower panels) for the years 2016, 2017 and 2018 (top to bottom) in the control (blue) and drought (orange) treatment. Shadings represent the 95% confidence intervals, and scatter in the background represents individual mean observations for each species and treatment ($n = 6$ trees per species and treatment). Asterisks and plus signs indicate differences between treatment intercepts with a p-value < 0.05 and p-value < 0.1, respectively ($n = 6$ trees per species and treatment). [Color figure can be viewed at wileyonlinelibrary.com]

principal component (PC) 1 in both species, which was mainly related to a negative relationship of MDS, which mainly reflects stem and especially cambium and phloem dehydration, and growth-related parameters (shoot and stem growth, end of growth, number of cells formed and cell width). While PC1 explained 30.6% of multi-variate variability in the data of *L. decidua*, a stronger association of these parameters with PC1 was found for *P. abies* (46.8% of multi-variate variability in the data), which suggests a stronger link between MDS and tree growth in this species.

4 | DISCUSSION

Our multi-year rain-exclusion experiment on mature trees at a subalpine forest site showed that, while differing in their water-use strategies, both *L. decidua* and *P. abies* strongly responded to drought. Drought responses were most pronounced as concerns growth and xylogenesis as well as stem tissue hydration, whereas xylem sap flow was less strongly affected. Drought effects were progressively amplified under recurrent drought, in spite of long winter seasons
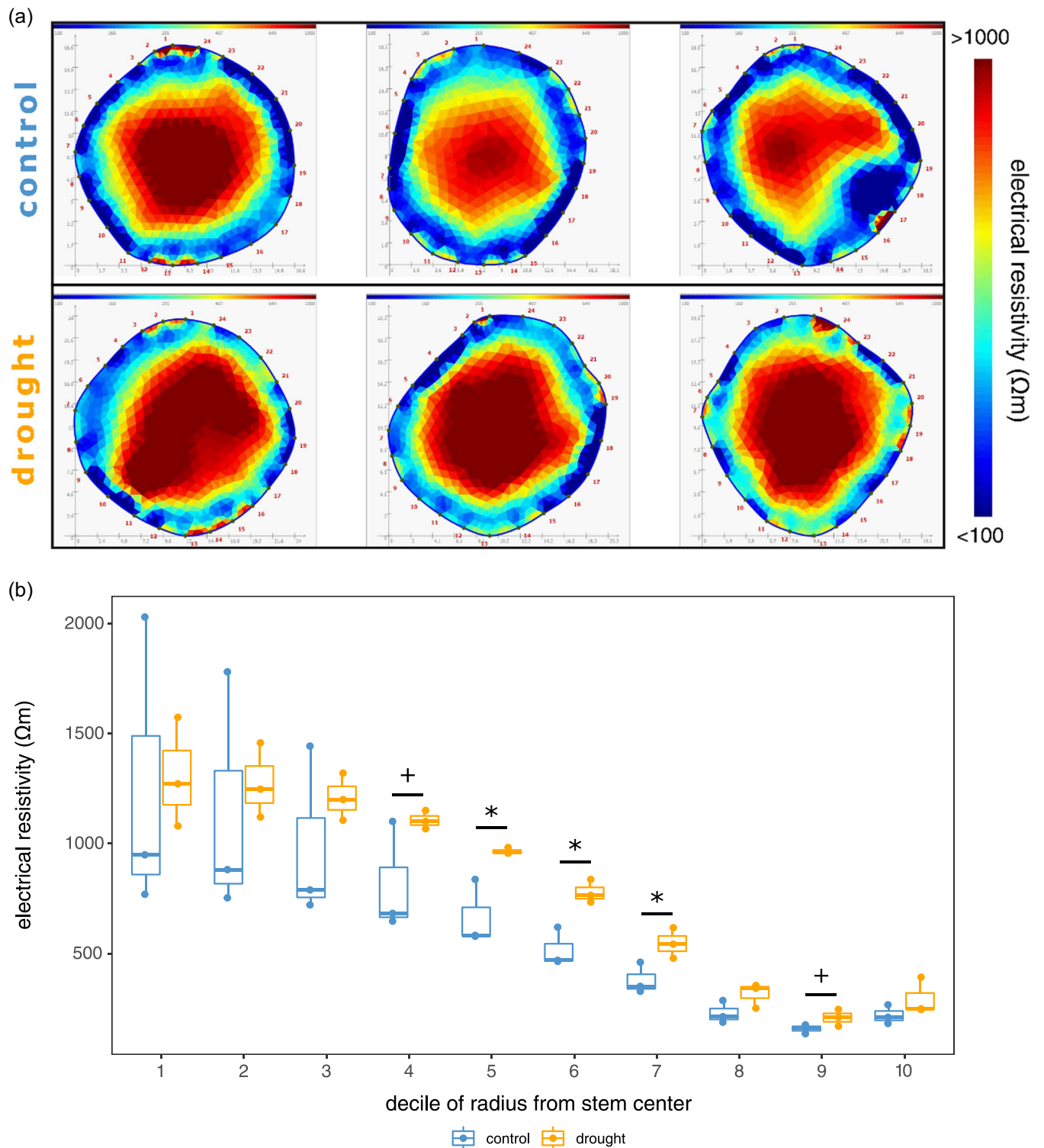
FIGURE 5 Electrical resistivity of *Picea abies* stems measured at peak drought in 2018. (a) Electrical resistivity tomograms of the trunk of three control trees (upper panel) and three drought exposed trees (lower panel) of *P. abies* measured at peak drought in 2018. In each tomogram, areas of high electrical resistivity are indicated by red colour while areas of low electrical resistivity are indicated by blue color. Note that the range of displayed electrical resistivity was set manually to 100–1000 Ωm to optimise visualisation. (b) Mean electrical resistivity (Ωm) for each decile along the stem radius from the stem centre (1st decile) to the stem periphery (10th decile). Colours denote treatment (control = blue, drought = orange). Points represent individual observations. Asterisks and plus signs indicate differences between treatments with a posterior probability >0.95 and >0.9, respectively (n = 3 per treatment). Note that electrical resistivity is inversely related to water content. [Color figure can be viewed at wileyonlinelibrary.com]
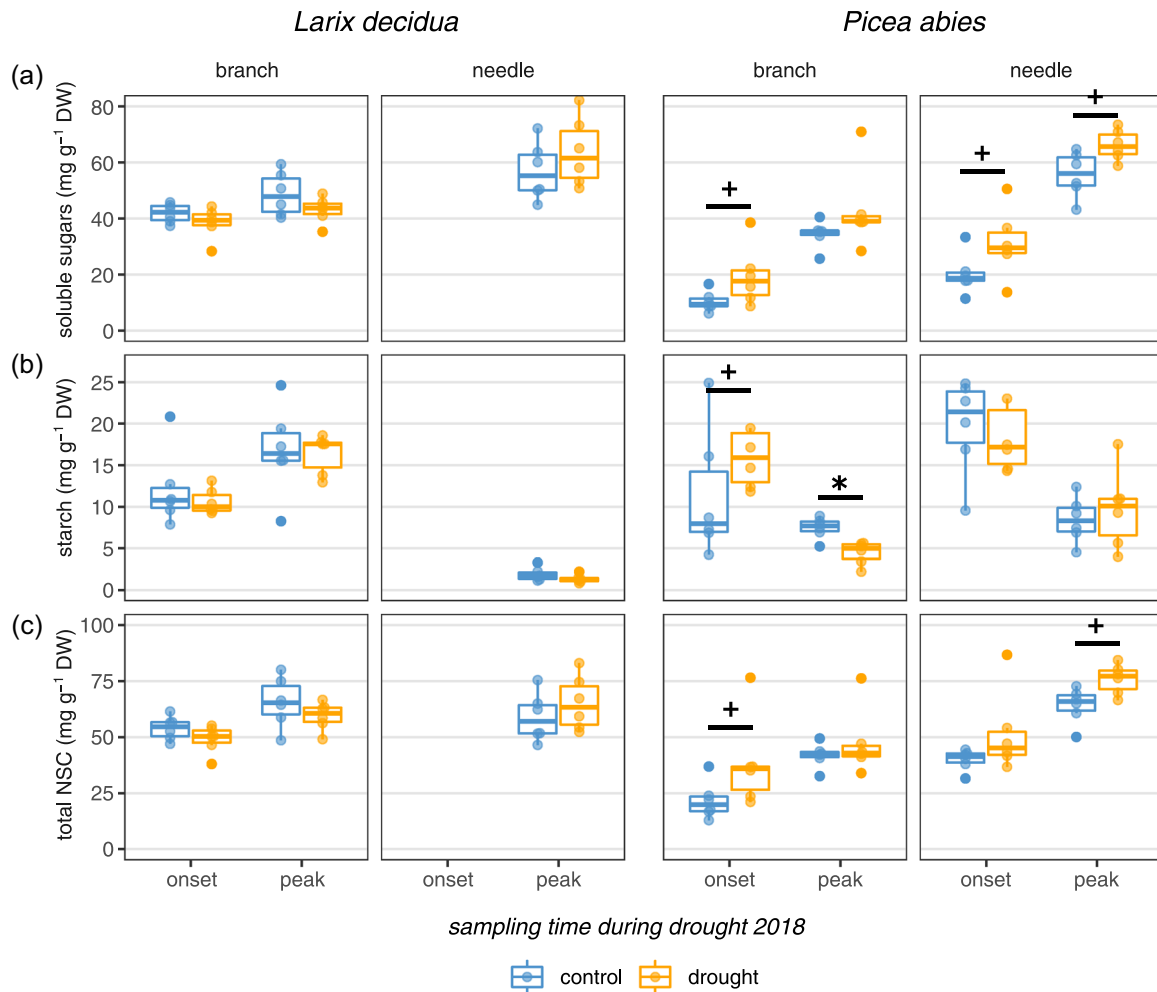
FIGURE 6 Concentrations of (a) soluble sugars, (b) starch and (c) total non-structural carbohydrates (NSC) measured in branches and needles in *Larix decidua* (left) and *Picea abies* (right). Samples were taken at the onset of drought (June) and at peak drought (September) in the third year of the drought treatment (2018). Colours denote treatment (blue = control, orange = drought). Boxplots denote median (bold horizontal line), 25th and 75th quartile (box) and 1.5 * interquartile range (whiskers). Points represent individual observations ($n = 6$ trees per species and treatment). Asterisks and plus signs indicate differences between treatments with a posterior probability >0.95 and >0.9, respectively. [Color figure can be viewed at wileyonlinelibrary.com]

during which soil water status was fully restored. Stem hydration dynamics were highly indicative of overall tree responses to drought, though their relationship with growth and NSC differed between the two species.

4.1 | Species-specific drought responses

L. decidua and *P. abies* have both been suggested to be sensitive to reduced soil moisture availability, especially at low to mid-elevations in xeric and mesic sites across the European Alps (e.g., Arend et al., 2021; Lévesque et al., 2013; Obojes et al., 2018). Compared to *L. decidua*, *P. abies* is generally considered the more drought-sensitive species, because it is more shallow-rooted and more conservative concerning its water use (Anfodillo et al., 1998; Hartl-Meier et al., 2014; Leo et al., 2014; Schmid & Kazda, 2002). It has also been shown that *L. decidua* downregulates stomatal conductance

more strongly than *P. abies* during atmospheric drought (Peters et al., 2019). Interestingly, in our study drought effects on xylem sap flow responses to VPD were similar in both species (Figure 4), which suggests a broadly similar stomatal sensitivity to VPD under reduced SWC. At the same time, under drought relative TWD was consistently larger in *L. decidua* (Figure 3, Supporting Information: Figure S7; Supporting Information: Table S4). This reflects more pronounced MDS in control trees of *P. abies* (Figure 3), but also indicates a more anisohydric behaviour of *L. decidua* under severely limiting soil moisture conditions. In spite of the larger TWDs, drought effects on xylem formation, in terms of xylem cell width and the number of cells formed, were less pronounced for *L. decidua* than for *P. abies* (Figure 2c,d). Studies showed that, on a diel scale, tree growth predominantly occurs during the night, when VPD is low and stem water is replenished (Chan et al., 2016; Zweifel et al., 2021), but there is also evidence that growth can peak in the afternoon (Mencuccini et al., 2017). In our study, stem hydration was similarly reduced by

FIGURE 7 δ¹³C of soluble sugars of *Larix decidua* (upper panels) and *Picea abies* (lower panels) sampled from branches (left) and needles (right) grown in 2018. Boxplots denote median (bold horizontal line), 25th and 75th quartile (box) and 1.5 * interquartile range (whiskers). Points represent individual observations. Colours denote treatment (blue = control, orange = drought). Asterisks and plus signs indicate differences between treatments with a posterior probability >0.95 and >0.9, respectively (*n* = 6 per species and treatment). [Color figure can be viewed at wileyonlinelibrary.com]
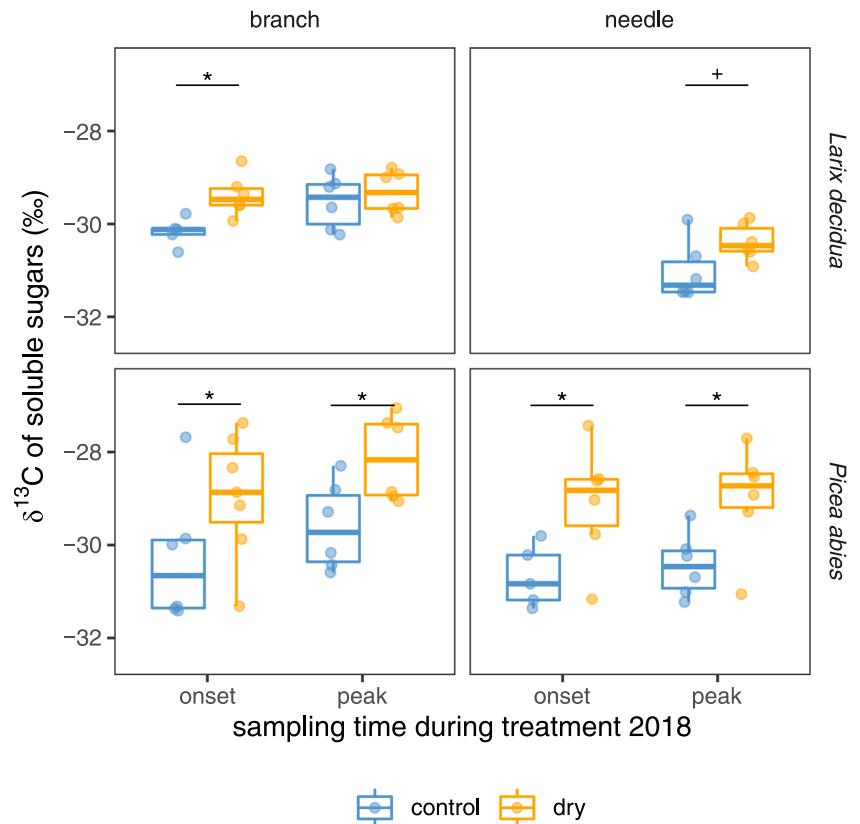
drought throughout the full diurnal cycle in both species (Figure 3), therefore differences in growth responses were likely related to diverging species-specific sensitivities to tissue water deficit. Given that turgor is the key determinant of cell formation and expansion rates (Cabon et al., 2020; Eilmann et al., 2009; Hsiao & Acevedo, 1974; Peters et al., 2021), species-specific differences in capacitance (Salomón et al., 2017, 2020), cell wall elasticity (Fan et al., 1994; Coussement et al., 2018) and regulation of tissue osmolality (Lintunen et al., 2016; Mencuccini et al., 2013; Paljakka et al., 2017; Peters et al., 2021), which affect turgor build-up and thus cell expansion, could have played a critical role.

L. decidua and *P. abies* also differed in their drought responses concerning NSC concentrations in branches and needles. While NSC concentrations in *L. decidua* were largely unaffected by drought, *P. abies* showed reduced starch concentrations in branches towards peak drought in the third year of drought (Figure 6, Supporting Information: S8). In addition, concentrations of NSC were higher in branches and needles of *P. abies* already at the onset of drought (Figure 6). This may have been caused by a shift in source-sink relations due to decreased growth in preceding years, but could also reflect an increased demand for osmoprotection (see below). Furthermore, less negative δ¹³C of soluble sugars in needles and branches at peak drought (Figure 7) indicates that intrinsic water-use efficiency of *P. abies* was more strongly increased under drought compared to *L. decidua*. Because an increase in δ¹³C and intrinsic water-use efficiency is strongly driven by a decrease in stomatal conductance under drought (Chaves et al., 2003; Flexas & Medrano, 2002; Lawlor & Tezara, 2009), our observation contrasts with recent findings on stomatal sensitivity to

drought for these two species (Peters et al., 2019). Increased intrinsic water-use efficiency has been previously observed in tree-rings formed in dry years, both in *L. decidua* and, to a stronger degree, *P. abies* (Lévesque et al., 2013; Lévesque et al., 2014). A recent tree-ring-based study also suggests that increased intrinsic water-use efficiency in another *Picea*-species was associated with a higher drought recovery potential (Wu et al., 2020).

In addition to our experiment on mature trees, we performed a drought experiment on saplings of *L. decidua* and *P. abies* growing in an open gap adjacent to our study site composed only of young trees, where precipitation was excluded during the same treatment periods. In contrast to what we found for mature trees, tree growth and the water use of saplings of both species was largely unaffected by the drought treatment (Wieser et al., 2019). This supports the notion that mature trees have a lower drought acclimation capacity than young and small trees (Fajardo et al., 2019; Olson et al., 2018). Because drought effects on saplings in subalpine forests are thus less pronounced, forest stand structure may change under future climate as a consequence of a higher drought vulnerability and species-specific differences of tall trees (Albrich et al., 2020; Bennett et al., 2015; Fajardo et al., 2019; Grote et al., 2016; McDowell et al., 2020; Stovall et al., 2019).

4.2 | Amplified responses under recurrent drought

While TWD was significantly increased by drought only in later summer of the first year of the experiment, it was clearly detectable in both species already from the onset of the drought treatments in

the second and third year (Figure 3, Supporting Information: Figure S7) and was associated with impaired xylogenesis and significant growth reductions (Figures 1a–f and 2, Supporting Information: Figure S4). Interestingly, even though the magnitude of MDS was similar in all the study years, dehydration effects on tree growth and its timing and on xylogenesis increased with recurrent drought. It is unlikely that the increased sensitivity of radial growth to TWD was due to progressive carbon limitation, given that leaves and branches had relatively constant levels of NSC under drought and that stem and roots may store substantial amounts of carbohydrates to sustain metabolism (Hoch et al., 2003; Rademacher et al., 2021; Rosell et al., 2021). Therefore, our findings suggest that the sensitivity of radial growth to TWD can increase under recurrent drought, which may be due to progressively decreasing stem hydraulic capacitance. Though its role under drought is not yet fully resolved (Körner, 2019), tree capacitance has been shown to decrease with drought stress (Salomón et al., 2017). Due to its lower relative volume, the contribution of water stored in the inner bark to stem hydraulic capacitance (Epila et al., 2017; Salomón et al., 2017) was likely limited in the species we studied. However, a reduction of the amount of water stored in the xylem could have played an important role, as suggested by the electrical resistivity tomography data for *P. abies* in the third year of drought (Figure 5). Multiple recurrent drought events could also decrease stem capacitance by reducing the diameter of xylem conduits (Figure 2; McCulloh et al., 2014). Furthermore changes in xylem anatomy, including pit anatomy, may affect the hydraulic conductivity and vulnerability to embolism (Gullo et al., 1995; Tyree & Ewers, 1991; Tyree & Sperry, 1989).

Because TWD is also linked to changes in phloem dehydration (Steppe et al., 2015), the observed MDS and TWD responses (Figure 3, Supporting Information: Figure S7) could indicate that phloem functioning was increasingly impaired under recurrent drought. Decreased phloem hydration is associated with low phloem turgor and high phloem sap viscosity, with direct consequences for tree carbon dynamics. Because the phloem functions as the main tissue for carbohydrate transport (Sevanto, 2014, 2018), impaired phloem transport can slow down C-supply to sinks (Ruehr et al., 2009; Salmon et al., 2019) and enhance a depletion of stored NSC in sink organs if local demand exceeds supply (Bréda et al., 2006; Dickman et al., 2015). Furthermore, carbon relocation across organs was shown to be hampered by drought (Hartmann, Ziegler, Kolle, et al., 2013; Hartmann, Ziegler, Trumbore, et al., 2013), thus remobilisation of stored carbon likely played a small role in NSC responses in branches and needles. As a result, the significant reduction in starch concentration in shoots during the third drought treatment (Figure 6, Supporting Information: Figure S8), which was similarly also reported for *P. abies* at a low elevation site exposed to a severe natural drought event (Arend et al., 2021), does not provide an indication of reduced phloem transport to sink organs. Because the concentrations of soluble sugars and total NSC were increased in needles and branches of drought-exposed *P. abies* (Figure 6), the reduction in starch content more likely reflected an active conversion to osmotically active sugars, and therefore a prioritisation of osmotic

regulation of water potential over C storage (Guo et al., 2020). The accumulation of osmotically active sugars has been observed repeatedly as a drought response in leaves, involving the conversion of starch as well as a preferential allocation of recently assimilated C to sugars (Chaves et al., 2003; Hartmann, Ziegler, Trumbore et al., 2013; Hasibeder et al., 2015; Nio et al., 2011). Interestingly, starch and soluble sugar concentrations in branches tended to be increased already at the onset of third drought treatment (reflected also in a significant increase in total NSC, Figure 6), which may result from greater reductions in growth than in photosynthesis under moderate drought conditions (McDowell et al., 2011). Furthermore, increased $\delta^{13}C$ of soluble sugars observed at the onset of the third drought in both species (Supporting Information: Figure S8) indicate a sustained imprint of previous drought treatments on intrinsic water-use efficiency (see above). Thus, recurrent drought had distinct legacies on tree C-water relations and overall C dynamics. Legacy effects of recurrent drought on radial growth may not only be due to decreased capacitance (see above), but could have also involved the legacy of an altered C balance in the previous year (Peters et al., 2017).

From previous studies based on natural drought events (Dietrich, Delzon, et al., 2018; Schuldt et al., 2020) and experimental droughts (He et al., 2020; Ježík et al., 2015; Zhang et al., 2018) we had expected a rapid response of xylem sap flow of both species to drought. However, in our experiment a significant reduction in xylem sap flow occurred only towards peak drought during the first 2 years and was distinct throughout the drought treatment only in the third year. Even under VPD levels at which no effects were observed in previous years and under comparatively low evaporative demand, in the third year of recurrent drought sensitivity of xylem sap flow to VDP was significantly increased (Figure 4), reflecting pronounced soil water controls on stomatal response (Carminati & Javaux, 2020; Cochard et al., 1996). This may have been partly caused by the exceptionally warm and dry summer of 2018, however, also clearly indicates a drought legacy in that xylem sap flow showed increased sensitivity to VPD already immediately after the start of the drought treatment when soil water potential was still comparatively high. There is only limited evidence from studies that suggest altered stomatal sensitivity to soil and plant water status under recurrent drought (e.g., Grossiord et al., 2018; Tombesi et al., 2018). Structural adjustments, as well as increasing limitations of root water uptake under recurrent drought, for example, caused by impaired root growth (Zwetsloot & Bauerle, 2021), decreased root functioning (Cuneo et al., 2016; Rodríguez-Calcerrada et al., 2017), reduced root mass (Meier & Leuschner, 2008), hydraulic disconnection from the soil (Carminati & Javaux, 2020; Carminati et al., 2009), as well as enhanced embolism in xylem conduits may have increased the sensitivity of transpiration to VPD under recurrent drought (Hammond, 2020; Mackay et al., 2020). Given the greater xylem dehydration observed in *P. abies* (Figure 5), an increased loss of hydraulic conductivity likely occurred at the peak of the third drought. It remains to be shown whether and to what degree under recurrent drought water loss of *L. decidua* and *P. abies* will be reduced through structural and physiological adjustments or through a loss of

hydraulic conductivity, the former decreasing and the latter increasing the risk of hydraulic failure.

4.3 | Conclusions

We conclude that recurrent drought amplified responses of *L. decidua* and *P. abies* to water stress by reducing tree water storage and the capacity of its replenishment, both on a diel and a seasonal timescale, with consequences for carbon relations including growth. While both species showed similar TWD responses, *P. abies* showed stronger growth responses to recurrent drought, reduced starch concentrations in branches and increased water-use efficiency when compared to *L. decidua*. Overall, our findings suggest that species differences in their growth responses to recurrent drought not only relate to the degree and dynamics of TWDs, but may also involve differences in turgor thresholds for growth, as well as differences in carbon-water relationships and the allocation of NSC to osmoregulation versus storage and growth. Increasing impacts of recurrent drought on tree carbon and water dynamics of both species suggest that increased drought frequencies could impose strong legacies with implications for the structure and functioning of mountain forests in a future climate.

CONFLICTS OF INTEREST

The authors declare no conflicts of interest.

DATA AVAILABILITY STATEMENT

All data that support the findings of this study are available at ZENODO data repository: https://doi.org/10.5281/zenodo.6553506.

ORCID

Florian Oberleitner http://orcid.org/0000-0001-7399-7428
Henrik Hartmann http://orcid.org/0000-0002-9926-5484
Jianbei Huang http://orcid.org/0000-0001-5286-5645
Adriano Losso http://orcid.org/0000-0001-7839-4941
Stefan Mayr http://orcid.org/0000-0002-3319-4396
Gerhard Wieser http://orcid.org/0000-0002-7575-5657
Michael Bahn http://orcid.org/0000-0001-7482-9776

REFERENCES

Adams, H.D., Collins, A.D., Briggs, S.P., Vennetier, M., Dickman, L.T., Sevanto, S.A. et al. (2015) Experimental drought and heat can delay phenological development and reduce foliar and shoot growth in semiarid trees. *Global Change Biology*, 21(11), 4210–4220.

Adams, H.D., Zeppel, M.J.B., Anderegg, W.R.L., Hartmann, H., Landhäusser, S.M., Tissue, D.T. et al. (2017) A multi-species synthesis of physiological mechanisms in drought-induced tree mortality. *Nature Ecology and Evolution*, 1(9), 1285–1291.

Albrich, K., Rammer, W. & Seidl, R. (2020) Climate change causes critical transitions and irreversible alterations of mountain forests. *Global Change Biology*, 26(7), 4013–4027.

Allen, C.D., Macalady, A.K., Chenchouni, H., Bachelet, D., McDowell, N., Vennetier, M. et al. (2010) A global overview of drought and heat-induced tree mortality reveals emerging climate change risks for forests. *Forest Ecology and Management*, 259(4), 660–684.

Allen, R.G., Pereira, L.S., Raes, D. & Smith, M. (1998) *Crop evapotranspiration-guidelines for computing crop water requirements-FAO Irrigation and drainage paper 56*. FAO.

Anderegg, W.R., Schwalm, C., Biondi, F., Camarero, J.J., Koch, G., Litvak, M. et al. (2015) Pervasive drought legacies in forest ecosystems and their implications for carbon cycle models. *Science*, 349(6247), 528–532.

Anderegg, W.R., Trugman, A.T., Badgley, G., Konings, A.G. & Shaw, J. (2020) Divergent forest sensitivity to repeated extreme droughts. *Nature Climate Change*, 10(12), 1091–1095.

Andivia, E., Ruiz-Benito, P., Díaz-Martínez, P., Carro-Martínez, N., Zavala, M.A. & Madrigal-González, J. (2020) Inter-specific tolerance to recurrent droughts of pine species revealed in saplings rather than adult trees. *Forest Ecology and Management*, 459, 117848.

Anfodillo, T., Rento, S., Carraro, V., Furlanetto, L., Urbinati, C. & Carrer, M. (1998) Tree water relations and climatic variations at the alpine timberline: seasonal changes of sap flux and xylem water potential in *Larix decidua* miller, *Picea abies* (L.) karst. and *Pinus cembra* L. *Annales des Sciences Forestières*, 55(1–2), 159–172.

Arend, M., Link, R.M., Patthey, R., Hoch, G., Schuldt, B. & Kahmen, A. (2021) Rapid hydraulic collapse as cause of drought-induced mortality in conifers. *Proceedings of the National Academy of Sciences of the United States of America*, 118(16), e2025251118.

Bahn, M., Knapp, M., Garajova, Z., Pfahringer, N. & Cernusca, A. (2006) Root respiration in temperate mountain grasslands differing in land use. *Global Change Biology*, 12(6), 995–1006.

Bär, A., Hamacher, M., Ganthaler, A., Losso, A. & Mayr, S. (2019) Electrical resistivity tomography: patterns in *Betula pendula*, *Fagus sylvatica*, *Picea abies* and *Pinus sylvestris*. *Tree Physiology*, 39(7), 1262–1271.

Bennett, A.C., McDowell, N.G., Allen, C.D. & Anderson-Teixeira, K.J. (2015) Larger trees suffer most during drought in forests worldwide. *Nature Plants*, 1, 15139.

Blumstein, M., Richardson, A., Weston, D., Zhang, J., Muchero, W. & Hopkins, R. (2020) A new perspective on ecological prediction reveals limits to climate adaptation in a temperate tree species. *Current Biology*, 30(8), 1447–1453.e1444.

Brandes, E., Kodama, N., Whittaker, K., Weston, C., Rennenberg, H., Keitel, C. et al. (2006) Short-term variation in the isotopic composition of organic matter allocated from the leaves to the stem of *Pinus sylvestris*: effects of photosynthetic and postphotosynthetic carbon isotope fractionation. *Global Change Biology*, 12(10), 1922–1939.

Bréda, N., Huc, R., Granier, A. & Dreyer, E. (2006) Temperate forest trees and stands under severe drought: a review of ecophysiological

responses, adaptation processes and long-term consequences. *Annals of Forest Science*, 63(6), 625–644.

Brooks, S.P. & Gelman, A. (1998) General methods for monitoring convergence of iterative simulations. *Journal of Computational and Graphical Statistics*, 7(4), 434–455.

Büntgen, U., Urban, O., Krusic, P.J., Rybníček, M., Kolář, T., Kyncl, T. et al. (2021) Recent European drought extremes beyond Common Era background variability. *Nature Geoscience*, 14(4), 190–196.

Bürkner, P.-C. (2017) brms: an R package for Bayesian multilevel models using stan. *Journal of Statistical Software*, 80(1), 1–28.

Bürkner, P.-C. (2018) Advanced Bayesian multilevel modeling with the R package brms. *The R Journal*, 10, 1.

Cabon, A., Fernandez-de-Una, L., Gea-Izquierdo, G., Meinzer, F.C., Woodruff, D.R., Martinez-Vilalta, J. et al. (2020) Water potential control of turgor-driven tracheid enlargement in Scots pine at its xeric distribution edge. *New Phytologist*, 225(1), 209–221.

Calanca, P. (2007) Climate change and drought occurrence in the alpine region: how severe are becoming the extremes? *Global and Planetary Change*, 57(1–2), 151–160.

Carminati, A. & Javaux, M. (2020) Soil rather than xylem vulnerability controls stomatal response to drought. *Trends in Plant Science*, 25(9), 868–880.

Carminati, A., Vetterlein, D., Weller, U., Vogel, H.-J. & Oswald, S.E. (2009) When roots lose contact. *Vadose Zone Journal*, 8(3), 805–809.

Cavender-Bares, J. & Bazzaz, F.A. (2000) Changes in drought response strategies with ontogeny in *Quercus rubra*: implications for scaling from seedlings to mature trees. *Oecologia*, 124(1), 8–18.

Čermák, J., Kučera, J. & Nadezhdina, N. (2004) Sap flow measurements with some thermodynamic methods, flow integration within trees and scaling up from sample trees to entire forest stands. *Trees*, 18(5), 529–546.

Chan, T., Holtta, T., Berninger, F., Makinen, H., Nojd, P., Mencuccini, M. et al. (2016) Separating water-potential induced swelling and shrinking from measured radial stem variations reveals a cambial growth and osmotic concentration signal. *Plant, Cell and Environment*, 39(2), 233–244.

Charra-Vaskou, K., Charrier, G., Wortemann, R., Beikircher, B., Cochard, H., Ameglio, T. et al. (2011) Drought and frost resistance of trees: a comparison of four species at different sites and altitudes. *Annals of Forest Science*, 69(3), 325–333.

Chaves, M.M., Maroco, J.P. & Pereira, J.S. (2003) Understanding plant responses to drought—from genes to the whole plant. *Functional Plant Biology*, 30(3), 239–264.

Cochard, H., Breda, N. & Granier, A. (1996) Whole tree hydraulic conductance and water loss regulation in Quercus during drought: evidence for stomatal control of embolism? *Annales des Sciences Forestieres*, 53, 197–206.

Cohen, J. (1988) *Statistical power analysis for the behavioral sciences*, 2nd edition, Hillsdale, NJ: Erlbaum.

Coussement, J.R., De Swaef, T., Lootens, P., Roldan-Ruiz, I., & Steppe, K. (2018) Introducing turgor-driven growth dynamics into functional-structural plant models. *Ann Bot*, 121(5), 849–861. doi:10.1093/aob/mcx144

Cuneo, I.F., Knipfer, T., Brodersen, C.R. & McElrone, A.J. (2016) Mechanical failure of fine root cortical cells initiates plant hydraulic decline during drought. *Plant Physiology*, 172(3), 1669–1678.

Dickman, L.T., McDowell, N.G., Sevanto, S., Pangle, R.E. & Pockman, W.T. (2015) Carbohydrate dynamics and mortality in a pinon-juniper woodland under three future precipitation scenarios. *Plant, Cell and Environment*, 38(4), 729–739.

Dietrich, L., Delzon, S., Hoch, G., Kahmen, A. & Battipaglia, G. (2018) No role for xylem embolism or carbohydrate shortage in temperate trees during the severe 2015 drought. *Journal of Ecology*, 107(1), 334–349.

Dietrich, L., Zweifel, R. & Kahmen, A. (2018) Daily stem diameter variations can predict the canopy water status of mature temperate trees. *Tree Physiology*, 38(7), 941–952.

Eilmann, B., Weber, P., Rigling, A. & Eckstein, D. (2006) Growth reactions of *Pinus sylvestris* L. and quercus pubescens willd to drought years at a xeric site in Valais, Switzerland. *Dendrochronologia*, 23(3), 121–132.

Eilmann, B., Zweifel, R., Buchmann, N., Fonti, P. & Rigling, A. (2009) Drought-induced adaptation of the xylem in Scots pine and pubescent oak. *Tree Physiology*, 29(8), 1011–1020.

Epila, J., De Baerdemaeker, N.J.F., Vergeynst, L.L., Maes, W.H., Beeckman, H. & Steppe, K. (2017) Capacitive water release and internal leaf water relocation delay drought-induced cavitation in African *Maesopsis eminii*. *Tree Physiology*, 37(4), 481–490.

Fajardo, A., McIntire, E.J.B. & Olson, M.E. (2019) When short stature is an asset in trees. *Trends in Ecology and Evolution*, 34(3), 193–199.

Fan, S., Blake, T.J., & Blumwald, E. (1994) The relative contribution of elastic and osmotic adjustments to turgor maintenance of woody species. *Physiologia Plantarum*, 90(2), 408–413. doi:10.1111/j.1399-3054.1994.tb00406.x

Flexas, J. & Medrano, H. (2002) Drought-inhibition of photosynthesis in C3 plants: stomatal and non-stomatal limitations revisited. *Annals of Botany*, 89(2), 183–189.

Francey, R. & Farquhar, G. (1982) An explanation of 13 C/12 C variations in tree rings. *Nature*, 297(5861), 28–31.

Ganthaler, A., Sailer, J., Bär, A., Losso, A. & Mayr, S. (2019) Noninvasive analysis of tree stems by electrical resistivity tomography: unraveling the effects of temperature, water status, and electrode installation. *Frontiers in Plant Science*, 10, 1455.

Gaylord, M.L., Kolb, T.E., Pockman, W.T., Plaut, J.A., Yepez, E.A., Macalady, A.K. et al. (2013) Drought predisposes pinon-juniper woodlands to insect attacks and mortality. *New Phytologist*, 198(2), 567–578.

Gelman, A. & Rubin, D.B. (1992) Inference from iterative simulation using multiple sequences. *Statistical Science*, 7(4), 457–472.

Gobiet, A., Kotlarski, S., Beniston, M., Heinrich, G., Rajczak, J. & Stoffel, M. (2014) 21st century climate change in the European Alps—a review. *Science of the Total Environment*, 493, 1138–1151.

Grams, T.E.E., Hesse, B.D., Gebhardt, T., Weikl, F., Rötzer, T. & Kovacs, B. et al. (2021) The Kroof experiment: realization and efficacy of a recurrent drought experiment plus recovery in a beech/spruce forest. *Ecosphere*, 12(3), e03399.

Grolemund, G. & Wickham, H. (2011) Dates and times made easy with lubridate. *Journal of statistical software*, 40(3), 1–25.

Grossiord, C., Buckley, T.N., Cernusak, L.A., Novick, K.A., Poulter, B., Siegwolf, R.T.W. et al. (2020) Plant responses to rising vapor pressure deficit. *New Phytologist*, 226(6), 1550–1566.

Grossiord, C., Sevanto, S., Limousin, J.-M., Meir, P., Mencuccini, M., Pangle, R.E. et al. (2018) Manipulative experiments demonstrate how long-term soil moisture changes alter controls of plant water use. *Environmental and Experimental Botany*, 152, 19–27.

Grote, R., Gessler, A., Hommel, R., Poschenrieder, W. & Priesack, E. (2016) Importance of tree height and social position for drought-related stress on tree growth and mortality. *Trees*, 30(5), 1467–1482.

Gullo, M.A., Salleo, S., Piaceri, E.C. & Rosso, R. (1995) Relations between vulnerability to xylem embolism and xylem conduit dimensions in young trees of quercus corris. *Plant, Cell and Environment*, 18(6), 661–669.

Günther, T. (2004) *Inversion methods and resolution analysis for the 2D/3D reconstruction of resistivity structures from DC measurements*. Universitätsbibliothek der TU BAF.

Günther, T., Rücker, C. & Spitzer, K. (2006) Three-dimensional modelling and inversion of DC resistivity data incorporating topography—II. Inversion. *Geophysical Journal International*, 166(2), 506–517.

Guo, J.S., Gear, L., Hultine, K.R., Koch, G.W. & Ogle, K. (2020) Non-structural carbohydrate dynamics associated with antecedent stem water potential and air temperature in a dominant desert shrub. *Plant, Cell and Environment*, 43(6), 1467–1483.

Hammond, W.M. (2020) *A matter of life and death: alternative stable states in trees, from xylem to ecosystems. Frontiers in Forests and Global Change*, 3.

Hanson, P.J., Todd, D.E., Jr. & Amthor, J.S. (2001) A six-year study of sapling and large-tree growth and mortality responses to natural and induced variability in precipitation and throughfall. *Tree Physiology*, 21(6), 345–358.

Hartl-Meier, C., Dittmar, C., Zang, C. & Rothe, A. (2014) Mountain forest growth response to climate change in the Northern limestone Alps. *Trees*, 28(3), 819–829.

Hartmann, H., Adams, H.D., Hammond, W.M., Hoch, G., Landhäusser, S.M., Wiley, E. et al. (2018) Identifying differences in carbohydrate dynamics of seedlings and mature trees to improve carbon allocation in models for trees and forests. *Environmental and Experimental Botany*, 152, 7–18.

Hartmann, H., Moura, C.F., Anderegg, W.R.L., Ruehr, N.K., Salmon, Y., Allen, C.D. et al. (2018) Research frontiers for improving our understanding of drought-induced tree and forest mortality. *New Phytologist*, 218(1), 15–28.

Hartmann, H., Ziegler, W., Kolle, O. & Trumbore, S. (2013) Thirst beats hunger - declining hydration during drought prevents carbon starvation in Norway spruce saplings. *New Phytologist*, 200(2), 340–349.

Hartmann, H., Ziegler, W., Trumbore, S. & Knapp, A.D. (2013) Lethal drought leads to reduction in nonstructural carbohydrates in Norway spruce tree roots but not in the canopy. *Functional Ecology*, 27(2), 413–427.

Hasibeder, R., Fuchslueger, L., Richter, A. & Bahn, M. (2015) Summer drought alters carbon allocation to roots and root respiration in mountain grassland. *New Phytologist*, 205(3), 1117–1127.

He, Q.Y., Yan, M.J., Miyazawa, Y., Chen, Q.W., Cheng, R.R., Otsuki, K. et al. (2020) Sap flow changes and climatic responses over multiple-year treatment of rainfall exclusion in a sub-humid black locust plantation. *Forest Ecology and Management*, 457, 117730.

Hoch, G., Richter, A. & Körner, C. (2003) Non-structural carbon compounds in temperate forest trees. *Plant, Cell and Environment*, 26(7), 1067–1081.

Holmes, R.L. (1983) Computer-assisted quality control in tree-ring dating and measurement. *Tree-Ring Bulletin*, 43, 69–78.

Hsiao, T.C. & Acevedo, E. (1974) Plant responses to water deficits, water-use efficiency, and drought resistance. *Agricultural Meteorology*, 14(1–2), 59–84.

Huang, J., Hammerbacher, A., Weinhold, A., Reichelt, M., Gleixner, G., Behrendt, T. et al. (2019) Eyes on the future—evidence for trade-offs between growth, storage and defense in Norway spruce. *New Phytologist*, 222(1), 144–158.

IPCC (2018) *Global Warming of 1.5°C. An IPCC Special Report on the impacts of global warming of 1.5°C above pre-industrial levels and related global greenhouse gas emission pathways, in the context of strengthening the global response to the threat of climate change sustainable development, and efforts to eradicate poverty*. IPCC.

Isaac-Renton, M., Montwé, D., Hamann, A., Spiecker, H., Cherubini, P. & Treydte, K. (2018) Northern forest tree populations are physiologically maladapted to drought. *Nature Communications*, 9(1), 5254.

Ježík, M., Blaženec, M., Letts, M.G., Ditmarová, Ľ., Sitková, Z. & Střelcová, K. (2015) Assessing seasonal drought stress response in Norway spruce (*Picea abies* L. Karst.) by monitoring stem circumference and sap flow. *Ecohydrology*, 8(3), 378–386.

Kahm, M., Hasenbrink, G., Lichtenberg-Fraté, H., Ludwig, J. & Kschischo, M. (2010) grofit: fitting biological growth curves with R. *Journal of Statistical Software*, 33(7), 1–21.

Kannenberg, S.A., Schwalm, C.R. & Anderegg, W.R.L. (2020) Ghosts of the past: how drought legacy effects shape forest functioning and carbon cycling. *Ecology Letters*, 23(5), 891–901.

Körner, C. (2003) Carbon limitation in trees. *Journal of Ecology*, 91(1), 4–17.

Körner, C. (2019) No need for pipes when the well is dry-a comment on hydraulic failure in trees. *Tree Physiology*, 39(5), 695–700.

Kröel-Dulay, G., Mojzes, A., Szitár, K., Bahn, M., Batáry, P., Beier, C. et al. (2022) Field experiments underestimate aboveground biomass response to drought. *Nature Ecology and Evolution*, 6, 540–545.

Kruschke, J.K. (2014) *Doing Bayesian data analysis: a tutorial with R, JAGS, and Stan*, 2nd edition, Burlington, MA: Academic Press.

Kruschke, J.K. (2013) Bayesian estimation supersedes the t test. *Journal of Experimental Psycholgy: General*, 142(2), 573–603.

Kruschke, J.K. (2018) Rejecting or accepting parameter values in Bayesian estimation. *Advances in Methods and Practices in Psychological Science*, 1(2), 270–280.

Lamacque, L., Charrier, G., dos Santos Farnese, F., Lemaire, B., Ameglio, T. & Herbette, S. (2020) Drought-induced mortality: branch diameter variation reveals a point of no recovery in lavender species. *Plant Physiology*, 183(4), 1638–1649.

Landhäusser, S.M., Chow, P.S., Dickman, L.T., Furze, M.E., Kuhlman, I., Schmid, S. et al. (2018) Standardized protocols and procedures can precisely and accurately quantify non-structural carbohydrates. *Tree Physiology*, 38(12), 1764–1778.

Lawlor, D.W. & Tezara, W. (2009) Causes of decreased photosynthetic rate and metabolic capacity in water-deficient leaf cells: a critical evaluation of mechanisms and integration of processes. *Annals of Botany*, 103(4), 561–579.

Leo, M., Oberhuber, W., Schuster, R., Grams, T.E.E., Matyssek, R. & Wieser, G. (2014) Evaluating the effect of plant water availability on inner alpine coniferous trees based on sap flow measurements. *European Journal of Forest Research*, 133(4), 691–698.

Lévesque, M., Saurer, M., Siegwolf, R., Eilmann, B., Brang, P., Bugmann, H. et al. (2013) Drought response of five conifer species under contrasting water availability suggests high vulnerability of Norway spruce and European larch. *Global Change Biology*, 19(10), 3184–3199.

Lévesque, M., Siegwolf, R., Saurer, M., Eilmann, B. & Rigling, A. (2014) Increased water-use efficiency does not lead to enhanced tree growth under xeric and mesic conditions. *New Phytologist*, 203(1), 94–109.

Lintunen, A., Paljakka, T., Jyske, T., Peltoniemi, M., Sterck, F., von Arx, G. et al. (2016) Osmolality and non-structural carbohydrate composition in the secondary phloem of trees across a latitudinal gradient in Europe. *Frontiers in Plant Science*, 7, 726.

Losso, A., Sailer, J., Bär, A., Ganthaler, A. & Mayr, S. (2020) Insights into trunks of *Pinus cembra* L.: analyses of hydraulics via electrical resistivity tomography. *Trees*, 34(4), 999–1008.

Mackay, D.S., Savoy, P.R., Grossiord, C., Tai, X., Pleban, J.R., Wang, D.R. et al. (2020) Conifers depend on established roots during drought: results from a coupled model of carbon allocation and hydraulics. *New Phytologist*, 225(2), 679–692.

Makowski, D., Ben-Shachar, M.S., Chen, S.H.A. & Ludecke, D. (2019) Indices of effect existence and significance in the Bayesian framework. *Frontiers in Psychology*, 10, 2767.

Martinez-Vilalta, J., Anderegg, W.R.L., Sapes, G. & Sala, A. (2019) Greater focus on water pools may improve our ability to understand and anticipate drought-induced mortality in plants. *New Phytologist*, 223(1), 22–32.

McCulloh, K.A., Johnson, D.M., Meinzer, F.C. & Woodruff, D.R. (2014) The dynamic pipeline: hydraulic capacitance and xylem hydraulic safety in four tall conifer species. *Plant, Cell and Environment*, 37(5), 1171–1183.

McDowell, N.G., Allen, C.D., Anderson-Teixeira, K., Aukema, B.H., Bond-Lamberty, B., Chini, L. et al. (2020) Pervasive shifts in forest dynamics in a changing world. *Science*, 368(6494).

McDowell, N.G., Beerling, D.J., Breshears, D.D., Fisher, R.A., Raffa, K.F. & Stitt, M. (2011) The interdependence of mechanisms underlying climate-driven vegetation mortality. *Trends in Ecology and Evolution*, 26(10), 523–532.

McDowell, N.G., Grossiord, C., Adams, H.D., Pinzón-Navarro, S., Mackay, D.S., Breshears, D.D. et al. (2019) Mechanisms of a coniferous woodland persistence under drought and heat. *Environmental Research Letters*, 14(4), 045014.

Meier, I.C. & Leuschner, C. (2008) Genotypic variation and phenotypic plasticity in the drought response of fine roots of European beech. *Tree Physiology*, 28(2), 297–309.

Mencuccini, M., Holtta, T., Sevanto, S. & Nikinmaa, E. (2013) Concurrent measurements of change in the bark and xylem diameters of trees reveal a phloem-generated turgor signal. *New Phytologist*, 198(4), 1143–1154.

Mencuccini, M., Salmon, Y., Mitchell, P., Hölttä, T., Choat, B., Meir, P. et al. (2017) An empirical method that separates irreversible stem radial growth from bark water content changes in trees: theory and case studies. *Plant, Cell and Environment*, 40(2), 290–303.

Menezes-Silva, P.E., Loram-Lourenco, L., Alves, R., Sousa, L.F., Almeida, S. & Farnese, F.S. (2019) Different ways to die in a changing world: consequences of climate change for tree species performance and survival through an ecophysiological perspective. *Ecology and Evolution*, 9(20), 11979–11999.

Meyer, S., Leifeld, J., Bahn, M. & Fuhrer, J. (2012) Free and protected soil organic carbon dynamics respond differently to abandonment of mountain grassland. *Biogeosciences*, 9(2), 853–865.

Moravec, V., Markonis, Y., Rakovec, O., Svoboda, M., Trnka, M., Kumar, R. et al. (2021) *Europe under multi-year droughts: how severe was the 2014–2018 drought period? Environmental Research Letters*, 16, 034062.

Müller, L.M. & Bahn, M. (2022) Drought legacies and ecosystem responses to subsequent drought. *Global Change Biology*.

Nio, S.A., Cawthray, G.R., Wade, L.J. & Colmer, T.D. (2011) Pattern of solutes accumulated during leaf osmotic adjustment as related to duration of water deficit for wheat at the reproductive stage. *Plant Physiology and Biochemistry*, 49(10), 1126–1137.

Obojes, N., Meurer, A., Newesely, C., Tasser, E., Oberhuber, W., Mayr, S. et al. (2018) Water stress limits transpiration and growth of European larch up to the lower subalpine belt in an inner-alpine dry valley. *New Phytologist*, 220(2), 460–475.

Olson, M.E., Soriano, D., Rosell, J.A., Anfodillo, T., Donoghue, M.J., Edwards, E.J. et al. (2018) Plant height and hydraulic vulnerability to drought and cold. *Proceedings of the National Academy of Sciences of the United States of America*, 115(29), 7551–7556.

Paine, C.E.T., Marthews, T.R., Vogt, D.R., Purves, D., Rees, M., Hector, A. et al. (2012) How to fit nonlinear plant growth models and calculate growth rates: an update for ecologists. *Methods in Ecology and Evolution*, 3(2), 245–256.

Paljakka, T., Jyske, T., Lintunen, A., Aaltonen, H., Nikinmaa, E. & Holtta, T. (2017) Gradients and dynamics of inner bark and needle osmotic potentials in Scots pine (*Pinus sylvestris* L.) and Norway spruce (*Picea abies* L. karst). *Plant, Cell and Environment*, 40(10), 2160–2173.

Peltier, D.M.P. & Ogle, K. (2019) Legacies of more frequent drought in ponderosa pine across the Western United States. *Global Change Biololgy*, 25(11), 3803–3816.

Pepin, N., Bradley, R.S., Diaz, H., Baraër, M., Caceres, E., Forsythe, N. et al. (2015) Elevation-dependent warming in mountain regions of the world. *Nature Climate Change*, 5(5), 424–430.

Peters, R.L., Klesse, S., Fonti, P. & Frank, D.C. (2017) Contribution of climate vs. larch budmoth outbreaks in regulating biomass accumulation in high-elevation forests. *Forest Ecology and Management*, 401, 147–158.

Peters, R.L., Speich, M., Pappas, C., Kahmen, A., von Arx, G., Graf Pannatier, E. et al. (2019) Contrasting stomatal sensitivity to temperature and soil drought in mature alpine conifers. *Plant, Cell and Environment*, 42(5), 1674–1689.

Peters, R.L., Steppe, K., Cuny, H.E., De Pauw, D.J.W., Frank, D.C., Schaub, M. et al. (2021) Turgor - a limiting factor for radial growth in mature conifers along an elevational gradient. *New Phytologist*, 229(1), 213–229.

Pilcher, J.R. (1990) Sample preparation, cross-dating and measurement. In: Cook, E.R. *Methods of dendrochronology*. Dordrecht: Kluwer, pp. 40–51.

Plaut, J.A., Yepez, E.A., Hill, J., Pangle, R., Sperry, J.S., Pockman, W.T. et al. (2012) Hydraulic limits preceding mortality in a piñon-juniper woodland under experimental drought. *Plant, Cell and Environment*, 35(9), 1601–1617.

Preisler, Y., Tatarinov, F., Grunzweig, J.M. & Yakir, D. (2021) Seeking the "point of no return" in the sequence of events leading to mortality of mature trees. *Plant, Cell and Environment*, 44(5), 1315–1328.

R Development Core Team. (2020) *R: a language and environment for statistical computing*. Vienna: R Foundation for Statistical Computing.

R Studio Team. (2020) *RStudio: integrated development for R*. Boston: RStudio, PCB.

Rademacher, T., Fonti, P., LeMoine, J.M., Fonti, M.V., Basler, D., Chen, Y. et al. (2021) Manipulating phloem transport affects wood formation but not local nonstructural carbon reserves in an evergreen conifer. *Plant, Cell and Environment*, 44(8), 2506–2521.

Rangwala, I. & Miller, J.R. (2012) Climate change in mountains: a review of elevation-dependent warming and its possible causes. *Climatic Change*, 114(3-4), 527–547.

Rennenberg, H., Loreto, F., Polle, A., Brilli, F., Fares, S., Beniwal, R.S. et al. (2006) Physiological responses of forest trees to heat and drought. *Plant Biology*, 8(5), 556–571.

Rodríguez-Calcerrada, J., Li, M., López, R., Cano, F.J., Oleksyn, J., Atkin, O.K. et al. (2017) Drought-induced shoot dieback starts with massive root xylem embolism and variable depletion of non-structural carbohydrates in seedlings of two tree species. *New Phytologist*, 213(2), 597–610.

Rosell, J.A., Piper, F.I., Jiménez-Vera, C., Vergílio, P.C., Marcati, C.R., Castorena, M. et al. (2021) Inner bark as a crucial tissue for non-structural carbohydrate storage across three tropical woody plant communities. *Plant, Cell and Environment*, 44(1), 156–170.

Rosner, S., Heinze, B., Savi, T. & Dalla-Salda, G. (2019) Prediction of hydraulic conductivity loss from relative water loss: new insights into water storage of tree stems and branches. *Physiologia Plantarum*, 165(4), 843–854.

Rücker, C., Günther, T. & Spitzer, K. (2006) Three-dimensional modelling and inversion of dc resistivity data incorporating topography—I. modelling. *Geophysical Journal International*, 166(2), 495–505.

Ruehr, N.K., Offermann, C.A., Gessler, A., Winkler, J.B., Ferrio, J.P., Buchmann, N. et al. (2009) Drought effects on allocation of recent carbon: from beech leaves to soil CO_2 efflux. *New Phytologist*, 184(4), 950–961.

Salmon, Y., Dietrich, L., Sevanto, S., Holtta, T., Dannoura, M. & Epron, D. (2019) Drought impacts on tree phloem: from cell-level responses to ecological significance. *Tree Physiology*, 39(2), 173–191.

Salomón, R.L., Limousin, J.M., Ourcival, J.M., Rodriguez-Calcerrada, J. & Steppe, K. (2017) Stem hydraulic capacitance decreases with drought stress: implications for modelling tree hydraulics in the Mediterranean oak *Quercus ilex*. *Plant, Cell and Environment*, 40(8), 1379–1391.

Salomón, R.L., Steppe, K., Ourcival, J.M., Villers, S., Rodríguez-Calcerrada, J., Schapman, R. et al. (2020) Hydraulic acclimation in a Mediterranean oak subjected to permanent throughfall exclusion results in increased stem hydraulic capacitance. *Plant, Cell and Environment*, 43(6), 1528–1544.

Sangines de Carcer, P., Vitasse, Y., Penuelas, J., Jassey, V.E.J., Buttler, A. & Signarbieux, C. (2018) Vapor-pressure deficit and extreme climatic variables limit tree growth. *Global Change Biology*, 24(3), 1108–1122.

Schmid, I. & Kazda, M. (2002) Root distribution of Norway spruce in monospecific and mixed stands on different soils. *Forest Ecology and Management*, 159(1–2), 37–47.

Schmitt, M., Bahn, M., Wohlfahrt, G., Tappeiner, U. & Cernusca, A. (2010) Land use affects the net ecosystem CO_2 exchange and its components in mountain grasslands. *Biogeosciences*, 7(8), 2297–2309.

Schuldt, B., Buras, A., Arend, M., Vitasse, Y., Beierkuhnlein, C., Damm, A. et al. (2020) A first assessment of the impact of the extreme 2018 summer drought on Central European forests. *Basic and Applied Ecology*, 45, 86–103.

Schwalm, C.R., Anderegg, W.R.L., Michalak, A.M., Fisher, J.B., Biondi, F., Koch, G. et al. (2017) Global patterns of drought recovery. *Nature*, 548(7666), 202–205.

Sevanto, S. (2014) Phloem transport and drought. *Journal of Experimental Botany*, 65(7), 1751–1759.

Sevanto, S. (2018) Drought impacts on phloem transport. *Current Opinion in Plant Biology*, 43, 76–81.

Spinoni, J., Vogt, J.V., Naumann, G., Barbosa, P. & Dosio, A. (2018) Will drought events become more frequent and severe in Europe? *International Journal of Climatology*, 38(4), 1718–1736.

Stan Development Team. (2020) Stan modeling language users guide and reference manual. Stan Development Team.

Steppe, K., Sterck, F. & Deslauriers, A. (2015) Diel growth dynamics in tree stems: linking anatomy and ecophysiology. *Trends in Plant Science*, 20(6), 335–343.

Stovall, A.E.L., Shugart, H. & Yang, X. (2019) Tree height explains mortality risk during an intense drought. *Nature Communications*, 10(1), 4385.

Tombesi, S., Frioni, T., Poni, S. & Palliotti, A. (2018) Effect of water stress "memory" on plant behavior during subsequent drought stress. *Environmental and Experimental Botany*, 150, 106–114.

Trugman, A.T., Anderegg, L.D.L., Shaw, J.D. & Anderegg, W.R.L. (2020) Trait velocities reveal that mortality has driven widespread coordinated shifts in forest hydraulic trait composition. *Proceedings of the National Academy of Sciences of the United States of America*, 117(15), 8532–8538.

Tyree, M.T. & Ewers, F.W. (1991) The hydraulic architecture of trees and other woody plants. *New Phytologist*, 119(3), 345–360.

Tyree, M.T. & Sperry, J.S. (1989) Vulnerability of xylem to cavitation and embolism. *Annual Review of Plant Physiology and Plant Molecular Biology*, 40(1), 19–36.

Valentini, R., Anfodillo, T. & Ehleringer, J.R. (1994) Water sources and carbon isotope composition (δ13C) of selected tree species of the Italian Alps. *Canadian Journal of Forest Research*, 24(8), 1575–1578.

Wickham, H., Averick, M., Bryan, J., Chang, W., McGowan, L.D.A., François, R. et al. (2019) Welcome to the tidyverse. *Journal of Open Source Software*, 4(43), 1686.

Wieser, G., Oberhuber, Gruber, Oberleitner, Hasibeder & Bahn, M. (2019) Artificial top soil drought hardly affects water use of *Picea abies* and *Larix decidua* saplings at the treeline in the Austrian Alps. *Forests*, 10(9), 777.

Wu, G., Liu, X., Chen, T., Xu, G., Wang, B. & Kang, H. et al. (2020) The positive contribution of iWUE to the resilience of Schrenk spruce (*Picea schrenkiana*) to extreme drought in the Western Tianshan Mountains, China. *Acta Physiologiae Plantarum*, 42(11), 1–16.

Zhang, Q., Jia, X., Shao, M., Zhang, C., Li, X. & Ma, C. (2018) Sap flow of black locust in response to short-term drought in Southern Loess Plateau of China. *Scientific Reports*, 8(1), 1–10.

Zuidema, P.A., Poulter, B. & Frank, D.C. (2018) A wood biology agenda to support global vegetation modelling. *Trends in Plant Science*, 23(11), 1006–1015.

Zuur, A.F., Ieno, E.N., Walker, N.J., Saveliev, A.A. & Smith, G.M. (2009) *Mixed effects models and extensions in ecology with R*. Springer.

Zweifel, R. (2016) Radial stem variations - a source of tree physiological information not fully exploited yet. *Plant, Cell and Environment*, 39(2), 231–232.

Zweifel, R., Haeni, M., Buchmann, N. & Eugster, W. (2016) Are trees able to grow in periods of stem shrinkage? *New Phytologist*, 211(3), 839–849.

Zweifel, R., Item, H. & Hasler, R. (2001) Link between diurnal stem radius changes and tree water relations. *Tree Physiology*, 21(12–13), 869–877.

Zweifel, R., Sterck, F., Braun, S., Buchmann, N., Eugster, W., Gessler, A. et al. (2021) Why trees grow at night. *New Phytologist*, 231(6), 2174–2185.

Zweifel, R., Zimmermann, L., Zeugin, F. & Newbery, D.M. (2006) Intra-annual radial growth and water relations of trees: implications towards a growth mechanism. *Journal of Experimental Botany*, 57(6), 1445–1459.

Zwetsloot, M.J. & Bauerle, T.L. (2021) Repetitive seasonal drought causes substantial species-specific shifts in fine-root longevity and spatio-temporal production patterns in mature temperate forest trees. *New Phytologist*, 231(3), 974–986.

SUPPORTING INFORMATION

Additional supporting information can be found online in the Supporting Information section at the end of this article.